Southern hemisphere thermohaline circulation stability and effect on global climate: results from coupled modeling

Author:
Trevena, Jessica

Publication Date:
2011

DOI:
https://doi.org/10.26190/unsworks/15231

Southern hemisphere thermohaline circulation stability and effect on global climate: results from coupled modeling

Jessica Trevena

Climate Change Research Centre, School of Mathematics and Statistics,

The University of New South Wales, Sydney, Australia

March 2011

Masters Thesis

A thesis submitted in fulfillment of the requirements for the degree of

Masters by Research

Originality Statement

'I hereby declare that this submission is my own work and to the best of my knowledge it contains no materials previously published or written by another person, or substantial proportions of material which have been accepted for the award of any other degree or diloma at UNSW or any other educational institution, expcept where due acknowledgment is made in the thesis. Any contribution made to the research by others, with whom I have worked at UNSW or elsewhere, is explicitly acknowledged in the thesis. I also declare that the intellectual content of this thesis is the product of my own work, except to the extent that assistance from others in the project's design and conception or in style, presentation and linguistic expression is acknowledged. '

Signed .....

Date .....

Copyright Statement

Signed .....

Date .....

Authenticity Statement

'I certify that the Library deposit digital copy is a direct equivalent of the final officially approved version of my thesis. No emendation of content has occurred and if there are any minor variations in formatting, they are the result of the conversion to digital format.'

Signed .....

Date .....

Abstract

This thesis investigates the stability of the Southern Hemisphere ocean thermohaline circulation, particularly the deepest branch, known as Antarctic Bottom Water (AABW), to Antarctic ice melt, and its role in the global thermohaline circulation (THC) in both present day and glacial climate states using a coupled climate model of intermediate complexity. The thesis is in two parts: in the first, present day experiments show AABW is stable to injections of freshwater (FW) from the Antarctic ice sheet equivalent to over 10m global sea level rise on centennial to millenial timescales, and does not have a stable 'off' state like the corresponding Northern Hemisphere THC - North Atlantic Deep Water (NADW). This is due to vastly different geographies, where zonally unrestricted Southern Hemisphere westerly winds drive Ekman pumping of salty Circumpolar Deep Water (CDW) largely independently of reduced thermohaline feedbacks during FW forcing, thus acting as a mechanism to resalinise surface oceans and reinvigorate AABW once FW forcing ceases. During times of FW intrusion however, AABW does temporarily 'switch off', causing local surface cooling, deep warming, decreases in oceanic northward heat transport and reductions in sea surface and surface air temperatures over the Southern Hemisphere mid-latitudes and tropics. The second part of the thesis aims to gain insight into the sensitivity of these results to base climate. A glacial simulation with ice sheets, atmospheric CO2 concentrations and orbital configurations like those of the Last Glacial Maximum, 21,000 years ago, is constructed, and similar experiments to Part 1 show the stability of the global THC has changed markedly. This is consistent with the colder and less stratified ocean, leading to a more fragile global THC where density differences between Southern and Northern Hemisphere overturning water-masses are smaller. Though AABW remains stable, FW anomalies propagating to the North Atlantic from the Antarctic can now dominate the bipolar density seesaw, switching the Northern Hemisphere THC into a different state where NADW reduces to zero and North Pacific Deep Water (NPDW) becomes dominant. This leads to extensive cooling over the North Atlantic and warming over the North Pacific and, to lesser extent, the Southern Ocean.

Acknowledgments

I would like to thank all who have supported me in completing this thesis and who have helped me with the emotional journey. I give particular thanks to my long-suffering supervisors Matthew England and Wenju Cai. Matt and Cai, your patience and enthusiasm are truly appreciated, I have learnt much and there will be more papers to come. I would also like to thank my past co-supervisor Willem Sijp, and Stephen Phipps for all their technical advice, as well as everyone in CCRC who offered answers to questions or support.

From a financial point of view, I thank University of New South Wales and CSIRO for allowing me the means to complete this research. I am also grateful for technical assistance from the National High Performance Computing Facility and various computing sections here on campus.

My parents, husband, grandparents, uncles and friends, Caroline, Andrea and Laura have been immensly supportive throughout the last number of years, and for that I thank them.

Preface

The aim of this thesis is to answer some questions that have been given much less attention than their Northern Hemisphere counterparts, regarding the sensitivity of the Southern Hemisphere climate to changes in the freshwater balance of the southern oceans. Changes in ocean freshwater balance drive climatic shifts by changing the stability of the water column, thus thermohaline circulation, ocean temperature and ultimately the overlaying atmosphere. Since observations of the Southern Ocean region point to greenhouse induced changes in this balance (Aoki *et al.*, 2003; Rintoul, 2007; Bindoff and McDougall, 2000; Jacobs *et al.*, 2002), such modeling studies have relevance to our understanding of the real climate system and its response to anthropogenic climate change.

Precipitation and land-ice melt from Antarctica are both sources of freshwater for the Southern Ocean; while changes in sea-ice volume, location and movement can change the distribution of freshwater over a region. In this thesis, we consider mainly land-ice - the freshwater source that has the potential to be the largest - to thus gauge the sensitivity of the modeled climate system and inform future experiments.

Past changes in ice mass balance are evident in the paleo record: on long, multi-million year timescales it is clear that there have been times in the Earth's history when no or very little ice existed at the poles and sea level varied by tens of metres (Katz *et al.*, 2008; Miller *et al.*, 2005). Physically based heuristic arguments of ice-sheet evolution, borne out by long-term ice mass balance modeling studies, indicate that the growth and decay of ice-sheets is non-linear, greatly accelerating once a threshold of warming or cooling is passed, due to the ice-albedo feedback and orbital changes (eg: De Conto and Pollard, 2003). On multi-millenial timescales, ^{14}C measurements taken in the Barbados region (Fairbanks, 1989) show evidence for periods of extremely rapid sea-level rise during the last 21 kyr. The most well known is meltwater pulse 1a (mwp1a), 14.6 kya, which added $15 - 25$ m to global sea level (GSL) (Gehrels, 2010) and was associated with GSL rise rates as high as $40 mmyr^{-1}$ (Stanford *et al.*, 2006). At least part of mwp1a is believed to have originated from Antarctica (Gehrels, 2010, and references therein), based on estimates of the amount of ice loss from the Antarctic Ice Sheet (AIS) since that Last Glacial Maximum (LGM), 21 kya. Ice core paleo-records obtained by the European Project

for Ice Coring in Antarctica (EPICA) Dome C project (Jouzel *et al.*, 2007) show distinct variations in temperature - linked to ice mass and extent - and Rohling *et al.* (2009) shows these are closely correlated to GSL, providing further support for Antarctic ice melt and sea-level linkages.

In recent years, ice melt or ice mass balance can be quantified by satellite and gravity anomaly measurements, and these repeatedly show that Antarctica is losing mass (Chen *et al.*, 2009; Velicogna and Wahr, 2006; Zwalley *et al.*, 2005; Davis *et al.*, 2005; Ramillien *et al.*, 2006; Rignot *et al.*, 2008), with a rare exception being Wingham *et al.* (2006), as shown in the comparison by Bentley *et al.* (2007). Studies that show a net ice loss over Antarctica as a whole unanimously find that the West Antarctic Ice Sheet (WAIS) is in negative mass balance, though the state of the East Antarctic Ice Sheet (EAIS) is less clear, being estimated as either in balance or slightly positive. Since this part of the ice sheet is better grounded, it is less affected by warming of the surrounding oceans, and therefore, it has been suggested, less susceptible to rapid breakdown (Thomas, 1979; Shepherd *et al.*, 2004).

Thus, there is a very good body of evidence pointing to a present net loss of land ice from the Antarctic, and a historical precedent for massive ice sheet collpase. Associated changes in freshwater balance would likely have large climatic impacts via thermohaline circulation changes, and yet interactive ice sheets are not included in the fully coupled models assessed in the IPCC report. Further, the observations on which ice mass balance calcuations depend are necessarily as short as the time that the technology has existed to aquire them - not much more than a decade - which is insufficient for identifying robust trends and Allison *et al.* (2009) notes *"the largest unknown in projections of sea level rise over the next century is the potential for rapid dynamic collapse of ice sheets."* Climatic responses to changing ice sheets thus have to be evaulated from other sources - paleo-records and, importantly, by other model simulations. Such studies are vital to improving our understanding of possible future climate scenario.

This modeling focus has been particularly marked in the North Atlantic, since the thermohaline circulation there (dominated by the North Atlantic Deep Water, NADW) shows 2 steady states in coupled climate models - on and off - that are associated with very different Northern Hemisphere climates (see Rahmstorf, 2002, and references therein). These 2 model states were first identified by Manabe and Stouffer (1988a), based on principles of salinity feedbacks proposed by Stommel (1961). Since then, paleo-proxies of NADW overturning strength have been shown

to have distinct variations that are closely correlated with temperature in Northern Hemisphere ice-core records, on many timescales, reflecting the likely reality of these 2 states and the linkage between NADW and Northern Hemisphere temperature, and thus ice mass (Clark *et al.*, 2002; Bond *et al.*, 1993). Such connections have generated much interest in NADW stability and how it affects and is affected by climate change - with the latest IPCC report finding it is very likely that NADW will slow during the 21st century.

The Southern Hemisphere, by contrast, has been largely neglected in investigations of this sort, despite it also having an overturning circulation. One of the main goals of this thesis is then to contrast the different behaviours in the Northern and Southern hemispheres in response to a high latitude freshwater forcing - why, physically, do they behave the same or differently? And what does this mean for probable responses to freshwater imbalances in the real world? This opened up many other side questions.

The thesis is divided into two parts. The first part focuses on the ocean response to high latitude freshwater anomalies using a coupled climate model of intermediate complexity (University of Victoria Coupled Climate Model, UVic CCM). The goal was to examine if the Southern Ocean also exhibits multiple stead states, given sufficient forcing, and if not, why not. This involved multiple experiments in which the Southern Ocean was forced with varying amounts of surface freshwater over varying timescales of the order of hundreds or thousands of years, simulating a rapid or slower Antarctic ice melt.

The second part of the thesis expands this work by looking at the response of the climate (in the same model) to similar perturbations when the base climate is different - namely, a glacial type climate. The idea for this experiment came about because changes in the Pacific ventilation have occurred around times of deglaciation (Ohkouchi *et al.*, 2002; Minoshima *et al.*, 2007), which appear to be anti-correlated with changes in the North Atlantic (Kiefer *et al.*, 2001; Saenko and Weaver, 2004). The North Pacific ventilation is much slower and shallower than the North Atlantic ventilation in the present climate, modifying the overlaying surface climate much less. We wanted to investigate if the system was similarly balanced when the ocean and climate as a whole were colder, and ocean stratification and ocean-atmosphere feedbacks were markedly different from the present day.

The work has been published in two journal articles, listed here:

Trevena, J., Sijp, W. P. and England, M. H., 2007: Stability of Antarctic Bottom Water Formation to Freshwater Fluxes and Implications for Global Climate. *Journal of Climate*, **21**, 3310-3326.

Trevena, J., Sijp, W. P. and England, M. H., 2008: North Atlantic Deep Water collapse triggered by a Southern Ocean meltwater pulse in a glacial climate state. *Geophysical Research Letters*, **35**, doi:10.1029/2008GL033236.

and is in the process of being expanded and extended upon in upcoming studies. The thesis concludes with some remarks on future studies.

Contents

List of Figures

Part I

Present day climate experiments

Chapter 1

AABW versus NADW stability

Abstract. The stability of Antarctic Bottom Water (AABW) to freshwater perturbations is investigated in a coupled climate model of intermediate complexity. It is found that AABW is stable to surface freshwater (FW) fluxes greater in volume and rate to those that permanently 'shutdown' North Atlantic Deep Water (NADW). Although AABW weakens during FW forcing, it fully recovers within 50 years of termination of FW input. This is due in part to a concurrent deep warming during AABW suppression that acts to eventually destabilise the water column. In addition, the prevailing upwelling of Circumpolar Deep Water (CDW) and northward Ekman transport across the ACC, regulated by the subpolar westerly winds, limits the accumulation of FW at high latitudes and provides a mechanism for re-salinifying the surface after the FW forcing has ceased. Enhanced sea-ice production in the cooler AABW suppressed state also aids in the re-salinification of the surface after FW forcing is stopped. Convection then restarts, with AABW properties only slightly colder and fresher compared to the unperturbed control climate state. Further experiments with larger FW perturbations, and with very slow application rates (0.2 Sv/1000 years), confirm the lack of multiple steady states of AABW in the model. This contrasts the North Atlantic, wherein classical hysteresis behaviour is obtained with similar forcing. The climate response to reduced AABW production is also investigated. During peak FW forcing, Antarctic surface sea and air temperatures decrease by a maximum of 2.5° C and 2.2° C respectively. This is of a similar magnitude to the corresponding response in the North Atlantic, although in the final steady-state, the AABW experiment returns to the original control climate, whereas the North Atlantic case transitions to a different steady-state characterised by substantial regional cooling (up to 6.0°C surface air temperature).

1.1. Introduction

Since Manabe and Stouffer (1988b) showed the existence of two different stable ocean circulation states under the same forcing in a global climate model, there have been numerous studies on the stability and variability of the global thermohaline circulation (THC) (see Rahmstorf *et al.* (2005) and references therein). The focus of virtually all of these studies has been on the North Atlantic Deep Water (NADW). The maintenance of two stable states of NADW is achieved via salinity feedbacks, as was clearly explained by Bryan (1986). To summarise, there is a thermal preference for high latitude sinking, but due to the additional dependence of density on salinity, it is possible to generate positive or negative feedbacks in the system via salt advection. In the North Atlantic case, the salinity feedback is positive. Freshwater (FW) addition over the sinking region will naturally inhibit convection. This results in a slowdown in the rate of flow of high salinity subtropical water to replace the sinking NADW. Thus, there is a positive feedback: if the FW perturbation is applied at a rate strong enough relative to the low latitude salt input, the original region of freshening becomes rapidly fresher and NADW shuts down.

The shutdown of NADW occurs despite a stabilising (or 'negative') thermal feedback which tends to make water that resides at the subpolar surface colder, and hence more dense. When NADW shutdown persists, the density increase due to this thermal effect is weaker than the density decrease due to surface freshening. This is a finely balanced system: if the initial salt and temperature forcings are different, then there is a different 'threshold' for NADW shutdown. The possibility of NADW collapse has sparked a number of studies on the response of the North Atlantic THC to global warming and/or Arctic sea-ice and Greenland ice sheet melt back and the effect this would have on climate (eg Stouffer and Manabe, 2003; Vellinga and Wood, 2002; Clark, 2002; Yin *et al.*, 2006; Prange *et al.*, 2001).

The Antarctic region's THC is likely to be subjected to enhanced glacial meltwater input over the coming years, however much less attention has been given to this region's water masses. The processes which maintain the deep THC are fundamentally different between the two hemispheres. In the North Atlantic, surface salt flows northward in the western boundary current of the North Atlantic subtropical gyre, resulting in the positive and negative feedback loops discussed above. In the Antarctic oceans by contrast, any geostrophic connection is 'blocked' by the Drake Passage gap where there is no 'western boundary' to permit geostrophically balanced flow. Surface meridional flow is northward via ageostrophic Ekman transport at the

latitudes of the Drake Passage gap, and the balancing deep return flow can only occur at depths where the presence of deep ocean ridges allows the north/south flow to be geostrophically balanced (Toggweiler and Samuels, 1995). Thus, the interaction between subpolar waters and subtropical saline waters does not occur directly via the subtropical gyres in the Southern Hemisphere. It is instead upwelled deep water that brings salt to the high latitudes of the Southern Hemisphere oceans, made up largely of outflowing NADW which is converted into Circumpolar Deep Water (CDW) (Goodman, 1998; Orsi *et al.*, 2001). The westerly winds control this upwelling of higher salinity CDW (Toggweiler and Samuels, 1993), a process which Goodman (1998) note is despite most of the global positive buoyancy forcing ocurring further north between $30°S$ and $30°N$. Once at the surface, strong heat loss to the atmosphere along with brine rejection during sea-ice formation transforms a significant portion of the upwelled water to higher densities, and it sinks along the Antarctic continental shelf, contributing to the bottom ventilating water-mass of the Southern Hemisphere - Antarctic Bottom Water (AABW). The importance of the westerly winds in maintaining this process was demonstrated by Toggweiler *et al.* (2006), who showed that a decrease in magnitude of the Southern Hemisphere westerly winds significantly reduced AABW formation rates (also noted by Rahmstorf and England, 1997; Saenko *et al.*, 2002). Toggweiler *et al.* (2006) also postulate that a northward shift of the winds would have a similar effect, via less upwelling of saline CDW, and because the upwelling of CDW would occur at lower, warmer latitudes, where transformation to dense AABW through heat loss to the atmosphere is less easily facilitated. This has recently been confirmed in a series of equatorward wind shift experiments by Sijp and England (2009). Another connection between the Antarctic and Southern Oceans can be via eddy transport, which operates particularly at the surface; though since the first quantification of these transports by Keffer and Holloway (1988), it has consistently been shown that meridional eddy salt transports in the region of the ACC are small compared to the mean flow transports, both in altimeter based observations (for eg: Wijffels, 2001) and in eddy resolving models (Lee *et al.*, 2006, ,their figure 7d). Meridional eddy heat fluxes however can be large (same references). Our study is concerned primarily with the response of long-term, balanced flows.

Another major difference between the Southern and Northern Hemispheres is the thermal isolation of Antarctica. This contributes to the formation of extensive areas of sea-ice over AABW formation regions, which injects salty brine into the surface ocean, helping maintain high surface densities and localised deep convective overturn (Orsi *et al.*, 1999), despite a largely stable halocline environment of the polar ocean (Keeling and Stephens, 2001).

The existence of multiple equilibria in the ocean's thermohaline circulation depends on a few critical ingredients. Firstly, the aforementioned 'positive' (salinity) and 'negative' (temperature) feedbacks need to act in competition at the region of water-mass formation. Secondly, in terms of salinity, the internal horizontal oceanic FW fluxes into the region of water-mass formation must be of opposite sign to the combined air-sea and ice-sea fluxes acting across the sea surface (e.g., Rahmstorf, 1996). This is required so that any collapse of the ocean overturning circulation is not re-invigorated by the buoyancy loss arising from both thermal and haline surface forcing. The above conditions are clearly met in the North Atlantic, wherein the northward advective salt fluxes act to oppose the prevailing surface freshening over the region's deep-water formation regions (the latter comes about via an excess of precipitation over evaporation). In contrast, with at least three regions of bottom water formation around the Antarctic continental margin, and limited direct observations of the surface ocean freshwater fluxes, it remains unclear whether multiple equilibria are possible for AABW. One of the main goals of the present study is to assess the possibility of multiple equilibria in the high-latitude Southern Ocean THC.

There have been limited studies of the stability and variability of AABW production to imposed climate change. Bi *et al.* (2001) examined the response of AABW to increasing atmospheric CO_2, finding that the surface ocean warming and enhanced hydrological cycle lead to a cessation of AABW production. However, once warming penetrates the deep ocean (in this case, after around 900 years), vertical density gradients return to close to control conditions, and convection and AABW formation is re-established. Bates *et al.* (2005) also examined the Southern Hemisphere response to atmospheric CO_2 increase, finding that the Antarctic Circumpolar Current (ACC) strengthens, and whilst AABW production initially decreases, it eventually recovers and actually increases, up from 12 Sv to 16 Sv. Brix and Gerdes (2003) examined the response of AABW to positive and negative salinity anomalies of 1 *psu* (practical salinity units) over the Weddell Sea, finding that AABW production naturally intensifies in the positive anomaly case, and weakens in the negative anomaly experiment. Interestingly, the negative salinity anomalies were observed to have a smaller influence on Antarctic and global overturning; although notably Brix and Gerdes (2003) used restoring boundary conditions, which inhibits the ocean-atmosphere and ocean-ice feedbacks that might have otherwise affected the response.

In contrast to the above studies, the goal here is to examine the stability of AABW in a pre-industrial climate using a global model that internally predicts surface ocean

freshwater fluxes. The response of AABW to varying FW perturbations will be examined in a global intermediate complexity climate model. This differs from most previous studies that have considered the AABW response to increased greenhouse gases, surface warming, imposed surface salinity changes and westerly wind strength changes. We do not include an interactive carbon cycle, as we wish to investigate the effects of temperature and salinity feedbacks on the Southern Hemisphere THC in isolation from carbon feedbacks. We explain the results in terms of the different salinity feedbacks operating in the global ocean and demonstrate that in the current climate model configuration, an AABW 'off' state is unstable. We also quantify the climate response to a transient slow-down in the AABW THC.

The rest of this paper is divided as follows: Section 2 outlines the model and experimental design, whilst Section 3 analyses the results, with an emphasis on the difference between the Antarctic and North Atlantic response to FW perturbations. Section 3 also includes the results of hysteresis experiments and the analysis of the climate response to FW perturbations. Finally, Section 4 covers a summary and conclusions of the main findings of the study.

1.2. Climate Model and Experimental Design

1.2.1. Climate Model

We use the University of Victoria Intermediate Complexity Climate (UVic) model, (Weaver *et al.*, 2001), suitable for multi-millenial simulations of the global climate system. The ocean model component has 19 depth levels, a resolution of 3.6 degrees longitude $\times$ 1.8 degrees latitude, and is coupled to a simple energy-moisture balance model of the atmosphere and a dynamic-thermodynamic model for sea-ice. The atmospheric model includes advection and diffusion of moisture, which has been shown to improve the global salinity distribution (Weaver *et al.*, 2001). The sea-ice model includes prediction of the ice thickness and ice area fraction in each grid cell, though it is only a single category sea-ice model. The brine beneath sea-ice is convected according to the parameterisation of Duffy and Caldeira (1997). Recently, a more realistic multi-category sea-ice model (Bitz and Lidcombe, 1999) has been incorporated into the UVic model, though we found no significant differences in the results using this newer multi-category sea-ice model. The climate model is linked to a prescribed Antarctic land-ice sheet that is static in time. Shelf mixing processes - whereby dense, saline surface water sinks to to the Antarctic continental shelf then overflows via density plumes into the deep ocean, is not resolved explicitly in the model. This is a common feature of global climate models suitable for

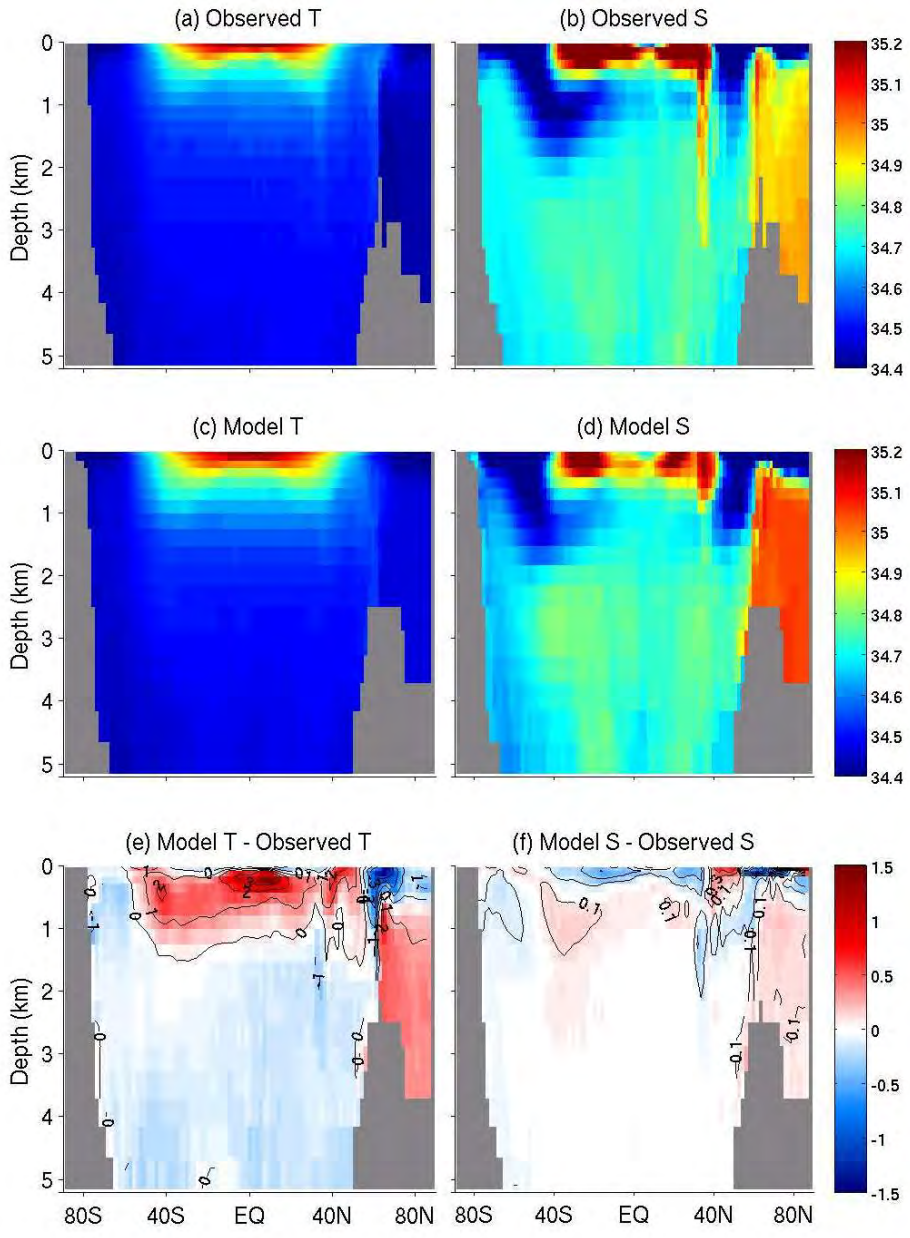

Figure 1.1. Observed temperature and salinity (top row) from Levitus *et al.* (1994). Model temperature and salinity (middle row) for the the CNTRL steady state. Anomaly (Model - Observed) for temperature (bottom left) and salinity (bottom right). Units are degrees Celsius and *psu*.

multi-millenial integrations. Such shelf processes depend on high resolution ocean physics and bottom bathymetry, which can only be parameterised in large-scale models. However, our focus is not on quantifying the variability of AABW, but on developing an understanding of basic salt feedback processes operating in the Antarctic and Southern Ocean regions at large scales.

Vertical diffusion varies according to the depth profile of Bryan and Lewis (1979), ranging from 0.3 cm^2s^{-1} beneath the surface mixed layer to 1.3 cm^2s^{-1} at the ocean bottom. The thickness of the surface ocean layer is 50 m, increasing to 500 m at the ocean abyss. Enhanced wind-driven surface mixing is approximated using a vertical diffusion coefficient of 1 cm^2s^{-1} and 0.5 cm^2s^{-1} in the top two layers. In addition, the ocean model incorporates the Gent and McWilliams (1990) parameterisation of eddy advection effects, implemented by way of an advection velocity acting on the tracer fields. We use identical isopycnal and isopycnal thickness diffusion coefficients of 4×10^6 cm^2s^{-1}, with a maximum isopycnal slope of 1 in 100. Although the isopycnal diffusion coefficients are quite low, experiments with higher coefficients of 2×10^7 cm^2s^{-1} showed no appreciable differences. It is known that vertical mixing is also important in determining deep overturning rates and their stability (see for example Sijp and England, 2006). In this study, we only consider different GM strengths, leaving a detailed sensitivity study of vertical diffusion to another study. The horizontal diffusion coefficient is set to zero throughout the global ocean. We use a constant lateral mixing coefficient for momentum of 2×10^9 cm^2s^{-1}, whilst the constant vertical mixing coefficient for momentum is 10 cm^2s^{-1}. The release of potential energy by convective overturning of the water column is modelled using the convective adjustment algorithm described by Rahmstorf (1993) (see also Pacanowski, 1995). A rigid-lid approximation is used and surface FW fluxes are modelled by way of an equivalent salt flux calculated using a fixed reference salinity.

The model is forced with present-day insolation, pre-industrial CO_2 of 280 ppm and present-day land-ice. Air and ocean temperature, as well as ocean salinity, are allowed to evolve freely. Wind is fixed within an annual cycle based on the monthly fields from the NCEP/NCAR reanalysis over the period 1958-1997 (Kalnay *et al.*, 1996), though to confirm the validity of our results, further experiments with wind feedbacks were also conducted. In the case of no wind feedback, the westerly winds overlying the ACC are unable to respond to changes in local sea surface temperatures, although it has recently been demonstrated that this feedback is weak (Sen Gupta and England, 2007).

The equilibrium control (CNTRL) state obtained with the above specifications generates approximately 21.0 Sv of NADW. Formation of AABW is characterised by a cell of strength 3.5 Sv, corresponding to overturning adjacent to Antarctica (Figure 1.2 inset). This apparently weak AABW overturning is however based on a zonal integral of vertical transport, which averages out downwelling and upwelling fluxes.

When downwelling and upwelling are considered separately to remove zonal aliasing, they amount to a net 11.4 Sv downwelling and 7.9 Sv upwelling south of 67.5° S at a depth of 1000 m (giving the net overturning maximum of 3.5 Sv). Deeper, at 2500 m, the net downwelling south of this latitude is 5.1 Sv; and this increases if we include latitudes further north up to 63.9°S. The model's AABW formation, measured in terms of net downwelling, is in reasonable agreement with the 8.1 Sv of AABW production determined by Orsi *et al.* (2001) using a chlorofluorocarbon-11 budget analysis. Another measure of the model's AABW strength, which depends less on aliasing, is the net northward flow of bottom water in the abyssal cell centred near 40° S (Figure 1.2 inset). This cell has strength 11.7 Sv in the CNTRL climate state, a similar strength to that seen in the CSIRO model used by Bi *et al.* (2001) (their Fig. 1a), and falls well within the range of model and observation based estimates of 4 Sv (Brix and Gerdes, 2003) to 27 Sv (Talley *et al.*, 2003).

A comparison of the zonal mean water properties in the CNTRL case with climatological (Levitus *et al.*, 1994) annual mean temperature and salinity fields shows that the model's AABW is slightly too fresh and cold, but within reasonable agreement of the observed. Globally averaged temperature and salinity (T-S) over the bottom layer of the ocean model are 0.77°C and 34.70 psu respectively compared to 0.91°C and 34.73 psu in the observed. The overall model T-S structure agrees well with the observed (Figure 1.1) and is comparable to IPCC (Intergovernmental Panel on Climate Change) class ocean climate models (see for example Griffies *et al.*, 2009). Apparent in the zonal mean is a tongue of low-salinity Antarctic Intermediate Water (AAIW) extending to depths greater than 1000 m in the mid-latitudes of the Southern Hemisphere. This overlays warm saline NADW in the Atlantic basin while abyssal cold, and fresher AABW is found in the deepest layers of the Atlantic, Pacific and Indian ocean abyss.

The model's zonally-integrated meridional salt transport (Figure not shown) indicates that, like the North Atlantic Ocean, the internal oceanic advective salt fluxes are poleward into the AABW formation regions. Thus, as described in Section 1.1, one necessary condition for the existence of multiple equilibria for AABW is satisfied. Concerning the other necessary condition, namely net FW gain via air-sea and ice-sea fluxes, the net surface fluxes are, for the most part, adding FW to the AABW formation regions, apart from a localised band of FW loss due to sea-ice formation along the highest latitude row of model grid points (Figure not shown). Thus, it is unclear that the second condition for multiple equilibria of AABW in the

model will be met. This will be explored further in Section 3.

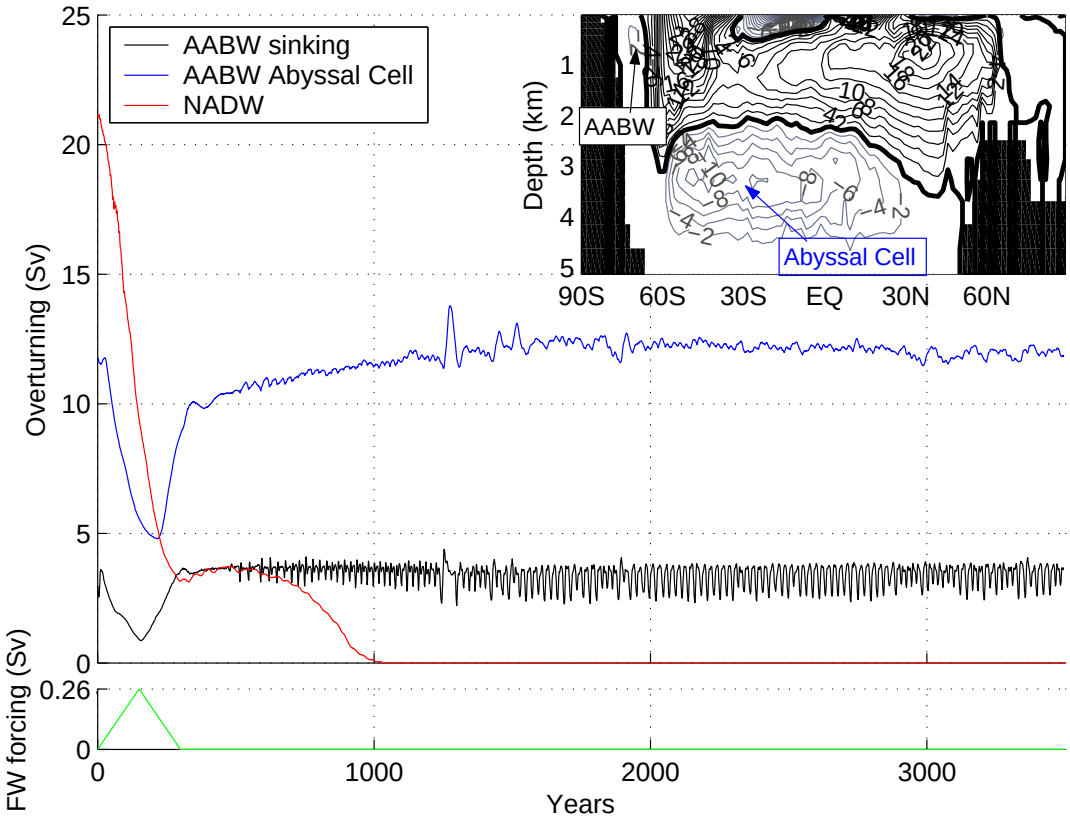

Figure 1.2. Overturning time series response to a 300 year symmetrical FW pulse, reaching a maximum rate of 0.26 Sv ($1\ Sv = 1 \times 10^6 m^3 s^{-1}$). Black curve indicates the zonally integrated AABW overturning adjacent to Antarctica; blue curve is the abyssal cell centred near $30 - 40°$ S; and the red curve is NADW overturning. The AABW curve are for experiment FW_{SO}, the NADW is for experiment FW_{NA}. Also shown in the inset is the initial condition (CNTRL) meridional overturning circulation (MOC) showing the location of the AABW cells plotted in the timeseries.

1.2.2. Experimental Design

We apply a positive FW flux to the ocean surface south of 63° S (Experiment FW_{SO}), that increases linearly at a rate of 0.004 myr^{-2} (see Figure 1.2 lower panel). This area encompasses the Ross and Weddell Seas, as well as almost the entire region where surface ocean potential temperature is less than $-0.5°$ C - the upper limit taken for many AABW studies (see for example Orsi *et al.*, 1999). The pulse is triangular in time, 300 years in length, increasing to a maximum value of 0.26 Sv at year 150, commonly above the threshold for NADW shutdown (eg: Rahmstorf *et al.*, 2005). Even pulses 5 times this size produced qualitatively similar results to those

presented below. For the corresponding North Atlantic experiment (FW_{NA}), we apply the FW flux between 51° N and 75° N over the Atlantic. The length of the pulse and volume of water applied in the FW_{NA} experiment are identical to those in FW_{SO}, though the areas differ (FW_{SO} covers approximately 2 times the area compared to FW_{NA}). We also repeated the FW_{SO} experiment with much larger FW pulses (up to a peak of 2 Sv), and obtained robust results to those presented below.

1.3. Results

1.3.1. Meridional overturning circulation

Figure 1.2 shows the time series of AABW and NADW in response to the FW pulse additions in FW_{SO} and FW_{NA}. For NADW, the measure is the maximum in the Atlantic sector meridional overturning streamfunction (see Figure 1.3b) north of 33° N. For AABW, there are two time series. The first is the minimum in the streamfunction between 63° S and Antarctica, and between 177 and 2497 m depth. The second is the bottom water outflow south of 33° S and below 2500 metres - otherwise known as the 'abyssal cell' due to its equivalence to the maximum zonally-integrated northward transport of bottom water. The location of both these cells is indicated in the inset of Figure 1.2.

During the period of the FW pulse in FW_{NA}, NADW decreases rapidly (Figure 1.2 red line), before showing what appears to be the beginning of a recovery after the FW addition period ends. The NADW cell then decreases again to reach zero by year 1000, where it remains stable for thousands of years. Thus, the North Atlantic overturning switches to a stable 'off' state in Experiment FW_{NA}. The overturning cell seen in the Northern Hemisphere in Figure 1.3g corresponds to overturning in the North Pacific, which develops when NADW is suppressed, consistent with the work of Saenko *et al.* (2004). In contrast, in Experiment FW_{SO}, the AABW sinking cell decreases to nearly zero (0.9 Sv) during the period of the pulse, but recovers within only 30 years after the FW flux ends, reaching a quasi-steady state value of 3.5 Sv. Although this appears to be a decrease of only 75 %, it should be remembered that this value is a measure of the minimum in the overturning streamfunction south of 63 S, which also shallows significantly during the pulse period, from 1000 m to 200 m (Figure 1.3a, c). When upwelling and downwelling are considered as a function of depth (see below), net downwelling decreases to zero in all but the top 200 m of the water column, showing that bottom water formation has essentially decreased

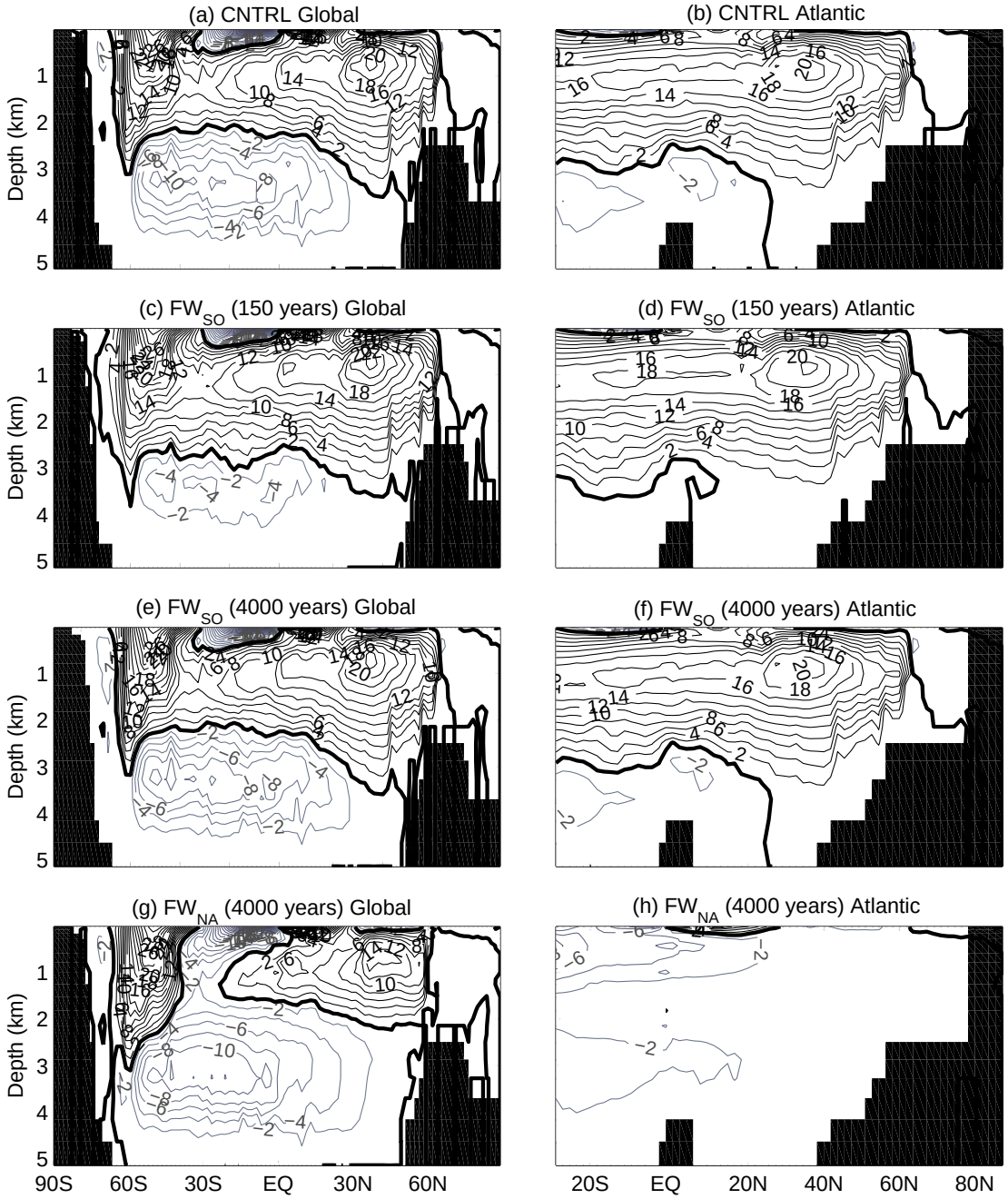

Figure 1.3. Final steady state meridional overturning circulation (MOC) for experiments CNTRL, FW_{SO} and FW_{NA} for the global (left) and Atlantic (right) oceans. Also shown is the MOC in FW_{SO} at the time of maximum AABW sinking response (150 yrs). Values are based on a 1-yr average and are given in Sv ($1\ Sv = 1 \times 10^6 m^3 s^{-1}$).

to zero. The abyssal cell also reduces during the period of the FW pulse, decreasing from 11.7 Sv to 4.8 Sv, only to recover back to just over 10 Sv by year 350, and to its control state value of 11.7 Sv by year 1000. After year 1000, the bottom water cell gradually increases to remain quasi-stable just above the control state at 12.0

Sv. The AABW sinking adjacent to Antarctica responds to the FW forcing within a decade or two, whilst the abyssal cell has a maximum response about 80 years after the maxima in the FW pulse. Given that the deep ocean typically responds on longer timescales than the more rapidly ventilated near surface layers, this is not surprising.

A third measure of AABW is obtained by decomposing the net upwelling and downwelling adjacent to Antarctica (Figure not shown), bearing in mind that the meridional overturning streamfunction is a zonal integral that aliases vertical motion. Though upwelling and downwelling decrease during the FW pulse period, downwelling decreases more, reducing from 11.4 Sv to 2.9 Sv at 1000 m, whilst upwelling decreases only from 7.9 Sv to 3.7 Sv at the same depth. Thus, by any measure AABW production slows in response to FW addition, but only temporarily before recovery to its pre-perturbation values. During FW_{SO}, NADW increases by 1.5 Sv during the period of the pulse, due to increased density contrasts between the Southern Ocean and the North Atlantic, which promote increased NADW production (Saenko *et al.*, 2003). After the pulse, NADW returns to its equilibrium value of 21.0 Sv. During FW_{NA}, AABW sinking decreases by less than 0.5 Sv. It appears that this is due to a reduction in the salinity of upwelled CDW in the Southern Ocean, though further studies are needed to confirm this. The abyssal cell strength shows an initial decrease of around 1.0 Sv during the period of NADW shutdown, before returning to close to its initial value a few centuries after NADW formation has reached zero. It should be noted that the AABW/NADW interaction is limited due to a deep Drake Passage in the present-day climate (see Sijp and England, 2005).

The final state meridional overturning streamfunctions for CNTRL, FW_{NA} and FW_{SO}, as well as for FW_{SO} at 150 years (the time of maximum AABW sinking response) are shown in Figure 1.3. During the period of the Southern Ocean FW pulse, AABW net sinking is almost entirely suppressed, and the deep outflow from the North Atlantic deepens and strengthens. The strengthening and deepening are associated with an increase in NADW overturning (1.7 Sv) and export into the Southern Ocean (1.8 Sv) while AABW is suppressed. This increase in NADW can be explained by increased surface Ekman transport of fresh water (originating from the imposed FW anomaly south of the ACC), where it causes AAIW to become fresher, less dense, and hence favour increased NADW sinking (see also Saenko *et al.*, 2003). NADW now fills - at least temporarily - more space in the abyss with the densest, bottom-most water mass in the world ocean (AABW) suppressed.

The final state meridional overturning streamfunctions in Figure 1.3 show that the

global and Atlantic overturning after 4000 years in FW_{NA} is significantly different from CNTRL, with a permanently collapsed NADW cell. On the other hand, FW_{SO} at 4000 years shows a state almost identical to CNTRL. The only noticable difference between FW_{SO} at 4000 years and CNTRL is a very slight northward extension of the AABW overturning adjacent to Antarctica, and a slightly deeper penetration of this cell. We hypothesise that this small departure of the final steady-state from CNTRL is due to additional FW now in the system. A lower salinity ocean leads to less stratification and thus deeper convection under the same surface forcing.

1.3.2. Water-mass properties

Zonal mean differences in T-S and a passive tracer for NADW are shown in Figure 1.4 at the height of the FW pulse (150 years) in experiments FW_{NA} and FW_{SO}. The passive tracer is applied with concentration unity at each time step to the ocean surface between 48° S and 66° N. If and when the water returns to the surface outside this domain, its concentration is reset to zero. When NADW is suppressed in FW_{NA}, the deep North Atlantic becomes cumulatively fresher due to a lack of salty water sinking (Keeling and Stephens, 2001), and salt accumulates in the surface ocean of the mid-latitudes (Figure 1.4b). The salinity decrease in the North Atlantic above 1500 m has a maximum zonal average value of 0.28 psu, whilst the zonal mean salinity increase at the surface mid-latitudes is up to 0.27 psu. The deep North Atlantic also cools during NADW suppression - by a maximum of 4.1° C (Figure 1.4d) - due to a lack of NADW sinking, and due to more ventilation now occuring via cold Southern Hemisphere water. The near surface mid-latitude Atlantic warms by 1.5° C (Figure 1.4d), with less tropical warm water pumped northward to replace sinking NADW. Stratification induced by the surface freshening in the North Atlantic leads to further freshening and stratification (via processes discussed in Section 1.1), which then leads to further suppression of NADW overturn, cooling the deep ocean further. Cooler Labrador Sea surface waters (up to 3.8° C) are subducted, contributing to the cooling seen in the shallow layers of the North Atlantic. A passive dye tracer injected into the North Atlantic surface shows a maximum zonal average decrease above 1500 m of 25% already by year 150 (Figure 1.4f), indicating the rapid decrease in production of this water-mass in experiment FW_{NA}. The increase in this tracer seen further south is due to less southward transport of NADW (not shown).

When AABW is suppressed in FW_{SO} the deep and bottom water T-S both increase, as shown in Figure 1.4a & c, and the surface Southern Ocean cools. Elsewhere

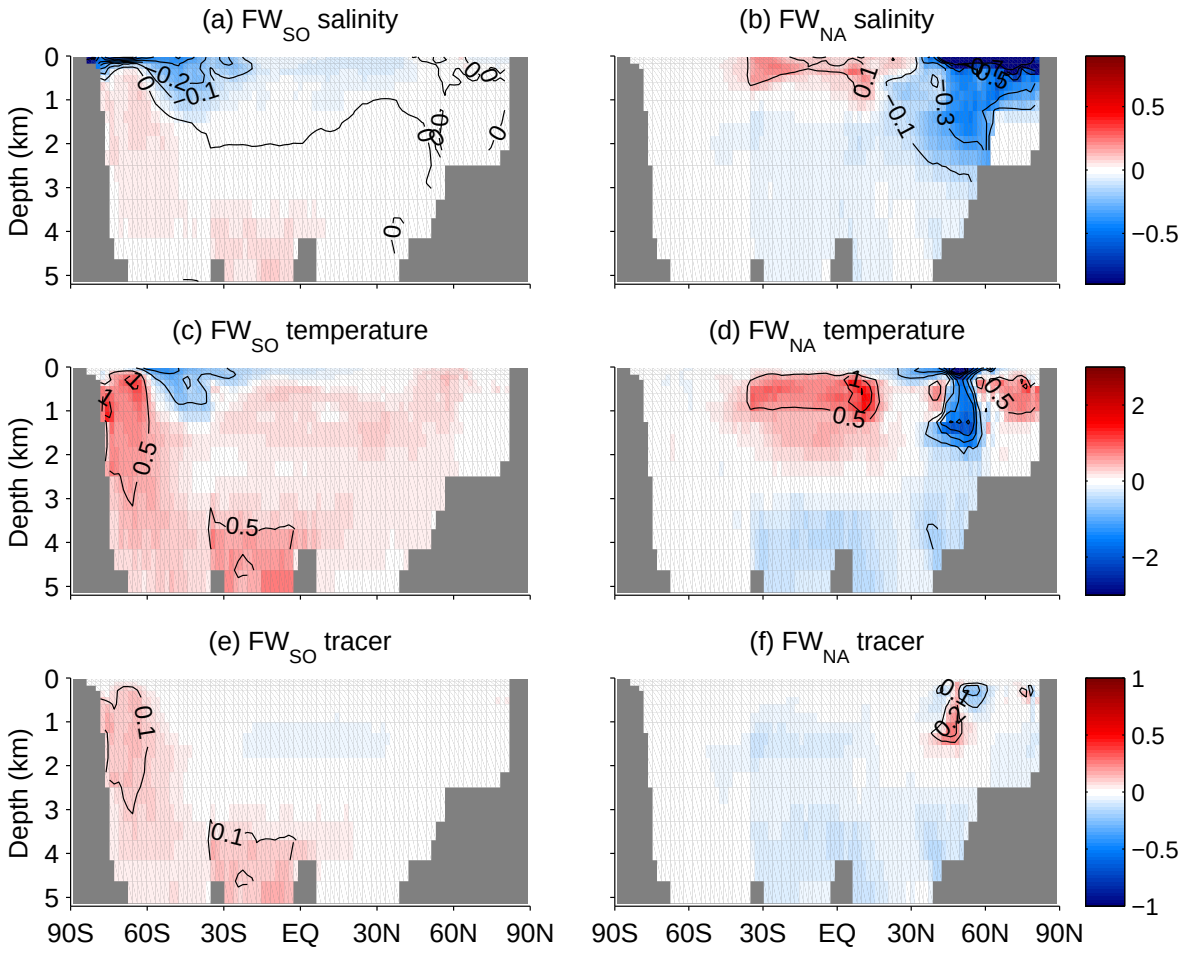

Figure 1.4. Zonally averaged difference fields (from CNTRL) for salinity, temperature and a passive NADW tracer for FW_{SO} (left) and FW_{NA} (right). The zonal mean includes the Atlantic basin plus a circumpolar average in the Southern Hemisphere south of 36.9° S. The data are averaged for 1 year at the height of the FW pulse (150 years). Note that the scale for each parameter is the same between experiments. Units are *psu*, degrees Celsius and fraction of tracer, respectively.

the ocean is little affected. Maximum zonally-averaged deep T-S differences (from CNTRL) between 500m and 2500 m depth are approximately 1.4° C and 0.09 *psu* respectively. The zonal-mean surface cooling and freshening is up to $-1.3°$ C and -1.1 *psu*. Both the deep T-S increase and the surface T-S decrease can be explained by less overturning of cold, fresh AABW into the interior. Suppressed convection over the AABW formation regions leads to less warm water being drawn upwards to replace the sinking water, forcing the deep ocean to warm, and the surface ocean to cool. This upwelling of warmer water provides a fundamental limit to sea-ice growth in the current Antarctic climate system (Goodman, 1998). Hence, in the suppressed state where this upwelling is significantly reduced, sea-ice grows compared to CNTRL (Figure 1.5a). Suppressed overturning of surface waters also prevents natural

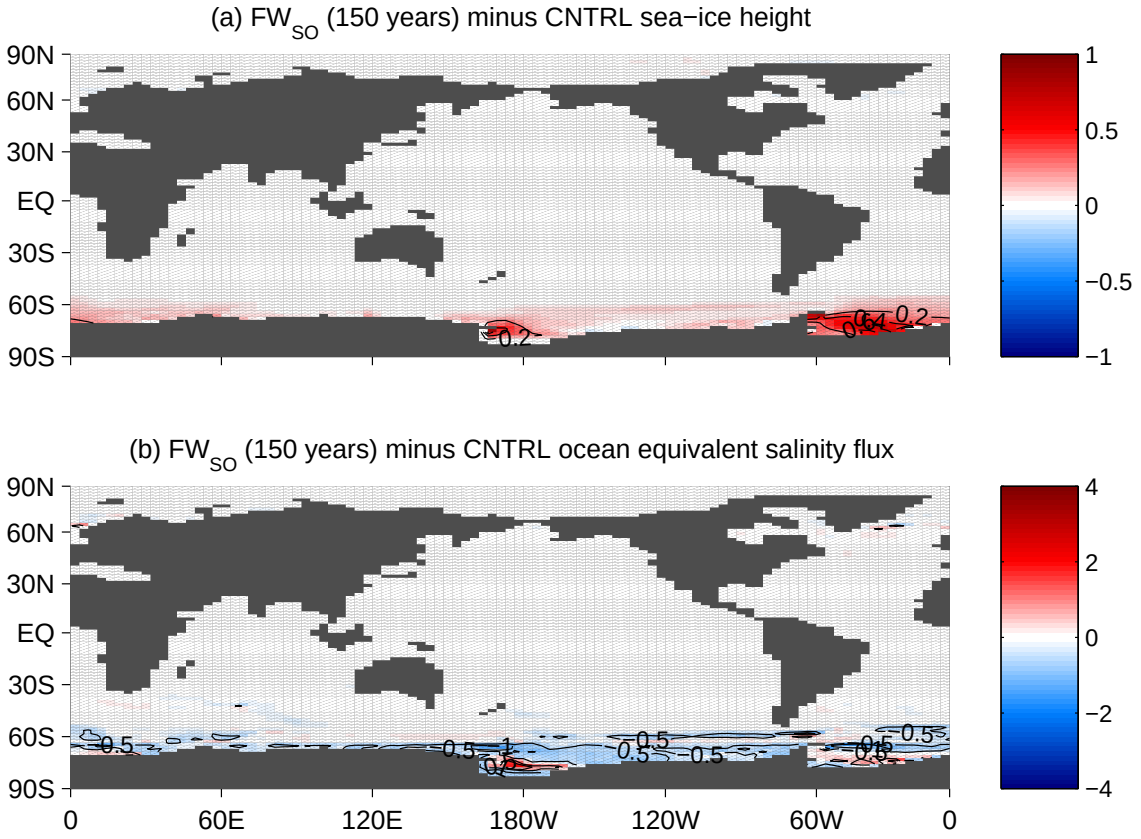

Figure 1.5. Difference in (a) sea-ice height and (b) equivalent surface salt fluxes for FW_{SO} at 150 years (difference from CNTRL). The equivalent ocean salt flux term includes E-P and sea-ice fluxes, but not the FW perturbation added to the Antarctic oceans. Positive values indicate increased sea-ice height and net salt flux into the ocean. All fields are based on a 1 year average. Units and contour interval are m and 0.2 m for (a) and $kgm^{-2}s^{-1}$ and 0.5 $kgm^{-2}s^{-1}$ for (b).

FW input, such as precipitation and summer meltwater, from mixing into the interior, thus further increasing the deep ocean salinity. The T-S changes in the deep ocean are also influenced by the increase in deep southward transport of warm saline NADW from the northern hemisphere (seen in Figure 1.3c & d). This warm, saline water is transported southwards across the ACC and upwelled around Antarctica, increasing the volume of relatively warm, saline water in the deep Antarctic ocean, and re-enforcing the T-S changes seen there.

While AABW is temporarily suppressed in FW_{SO} more of the ocean's deep and bottom water is sourced from the North Atlantic, at the expense of the Antarctic source regions. This is confirmed in an analysis of the difference in concentration of a North Atlantic passive tracer at 150 years between FW_{SO} and CNTRL (Figure 1.4e). At depths greater than a few hundred metres, the passive tracer shows

a maximum zonal average increase of up to 18 % already by year 150. This increase is due both to an increase in NADW sinking and production which is then transported into the ACC to comprise CDW, and to a reduction in the amount of AABW overturned locally within the Southern Ocean. Both these effects act to increase the volume of saline NADW in the deep and bottom ocean south of the ACC.

The deep warming in FW_{SO} reduces the stability of the water column, whilst the deep salinity increase tends to stabilise it. Relative to CNTRL, increased surface salinity fluxes from sea-ice and steady vertical ocean salt transport (CDW upwelling) during AABW suppression (Figure 1.5b), weaken the stability of the water column by the end of the FW pulse (seen later in Figure 1.7a). Indeed, Figure 1.6b, which will be discussed in more detail in Section 1.3.3, shows that soon after the FW forcing has ceased, surface salinities increase above that of CNTRL, and convection and overturning restart as seen in Figure 1.2.

Closer examination of Figure 1.2 shows that the overturning response follows soon after the changes in the FW pulse - indicating a nearby salt source which prevents FW accumulation in the area around Antarctica. In the current climate, the accumulation of FW from high precipitation rates over the Southern Ocean is prevented by efficient northward Ekman transport of the surface FW (in the form of both water and sea-ice). This transport constitues a net positive salt flux over AABW formation regions, important for AABW maintenance (Saenko and Weaver, 2001; Orsi *et al.*, 1999). In addition to the northward Ekman transport, positive salt fluxes from the upwelling of saline CDW are also known to be important for maintaining AABW formation (Goodman, 1998; Toggweiler *et al.*, 2006). The combination of upwelling saline CDW, together with the northward Ekman transport of FW can, together, be seen as a 'flushing' mechanism for the high latitude Southern Ocean, whereby salt is constantly returned, and FW constantly removed (see the schematic in Figure 1.6a). Most importantly, these two processes persist during the period of FW perturbation, in distinct contrast to the North Atlantic, wherein a FW addition can collapse the poleward salt transport replenishment process. This fundamental difference between the Antarctic and North Atlantic oceans provides an explanantion for the observed stability of AABW seen in the model.

1.3.3. Mechanisms removing the Southern Ocean FW anomaly

It is argued above that the upwelling of CDW provides a constant source of salinity to the high latitude Southern Ocean, that persists regardless of FW perturbations.

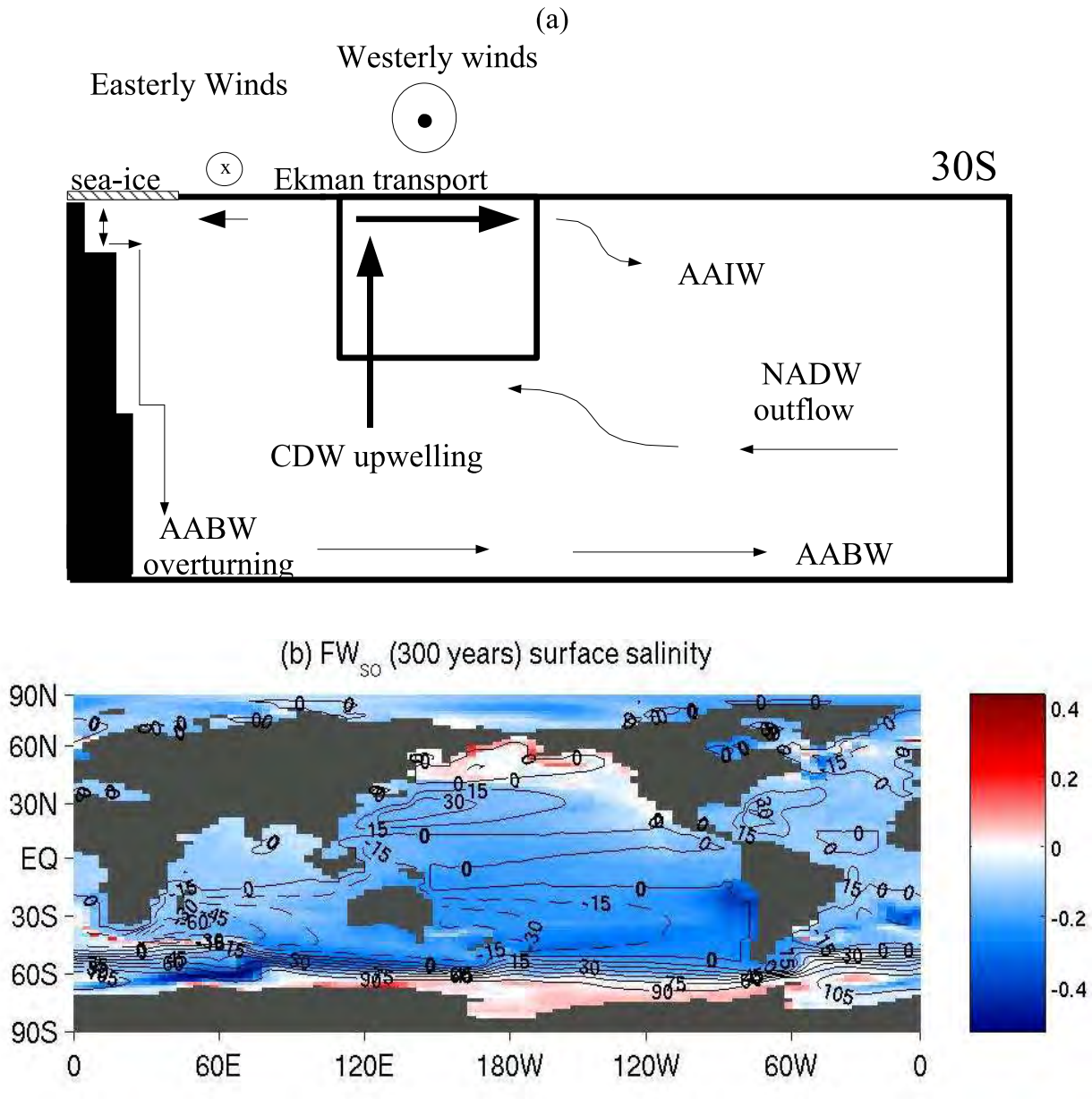

Figure 1.6. (a) Schematic diagram showing the Southern Ocean thermohaline and wind-driven circulation described in the text. (b) FW_{SO} salinity difference from CNTRL at 300 years with overlaid contours of ocean barotropic transport strength in Sverdrups (Sv), showing a clear demarcation of the high latitude enhanced salinity area. Contour interval is 15 Sv. All values are based on a 1 year average.

With winds fixed in the model, this is easy to demonstrate as the equation for wind driven upwelling,

$$w = \frac{\nabla \times \tau}{f\rho} \tag{1.1}$$

(where τ = horizontal wind stress, f = the Coriolis parameter and ρ = ocean water density) shows a negligible dependence on ocean density, as ρ appears in the denominator. We have made the approximation that f is constant, which is commonly done (Gill, 1982) as the Coriolis force varies more slowly than wind stress in the region of the Drake Passage. In the real system, FW anomalies could trigger circulation changes that feedback to alter the wind field, thus affecting CDW upwelling as per Equation (1). To assess this, similar experiments are conducted in which a wind feedback is employed. In such experiments, Ekman pumping changes also remain weak, with changes in w no more than in the experiments where there is no wind feedback.

Northward Ekman velocities v out of the high latitude Southern Ocean also remain nearly constant during FW_{SO} (Figure not shown), changing by less than 5%. When repeating the experiments with the model's wind feedback enabled, Ekman transport changes are at most 10%. Since the northward Ekman velocity remains similar, but the transported water is much fresher, the net equivalent salt transport returning to the high-latitude Southern Ocean increases in response to the FW anomaly. This enables a mechanism of removing the added FW perturbation that is independent of AABW sinking.

To summarise, the 'flushing' combination of wind-driven upwelling and meridional Ekman transport remains steady during FW_{SO}, removing added FW from the high-latitude Southern Ocean surface, (as also seen by Stouffer *et al.*, 2007), and providing a salt source to it, both of which are largely independent of the AABW sinking rate. Repeating these experiments with an ocean-atmosphere wind-feedback enabled did not alter these results. Though this 'flushing' is insufficient to maintain AABW sinking during the FW perturbation phase, once FW addition has ceased, the surface salinities return close to, or even greater than those in CNTRL (Figure 1.6b), and convection and overturning restart (Figure 1.2). Figure 1.6b shows that by year 300, the added FW has been mostly dispersed to the north of the ACC, except in parts of the Weddell Sea and in the Indian Ocean sector of the Antarctic waters. A region of increased salinity in the high latitude Southern Ocean is bordered to the north by the ACC. Since wind-driven upwelling is most efficient over the region of the ACC (Toggweiler *et al.*, 2006), this further supports the significance of the winds in the re-initation of AABW sinking. Finally, we explored further sensitivity experiments wherein the winds were shifted north by 4° to 6° latitude (hence the upwelling of salty CDW is also shifted further north). These experiments

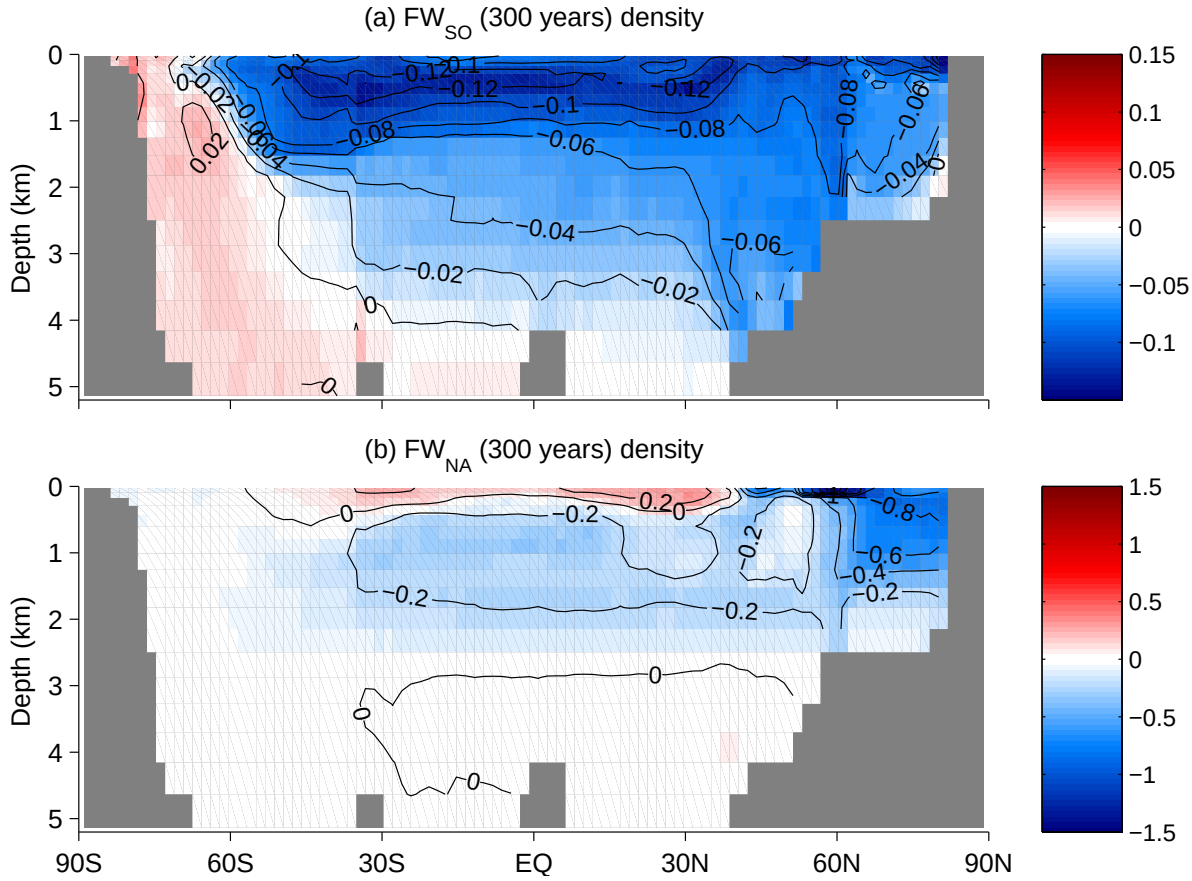

Figure 1.7. Zonally-averaged difference in density (from CNTRL) in FW_{SO} and FW_{NA} at the end of the FW pulse period (300 years). The zonal-average includes the Atlantic basin plus a circumpolar area in the Southern Hemisphere south of 36.9° S. The data are averaged for 1 year at the end of the pulse period. The reference pressure is 2500 dbar. Note that the scale for FW_{SO} is a factor of 10 less than that for FW_{NA}. Contour interval is 0.02 kgm^{-3} in (a) and 0.2 kgm^{-3} in (b).

showed recovery of AABW after the FW pulse is terminated, only there is a slower recovery time as the FW removal mechanism is less efficient.

In addition to the advective salt fluxes from vertical and horizontal ocean velocities, changes in surface processes also play a role in increasing the surface salinity once the FW pulse ends. At 150 years in FW_{SO}, despite the constant surface dilution by the FW anomaly, surface salt fluxes over the Ross and Weddell Seas decrease less than over the other regions of the Southern Ocean. Figure 1.5b shows surface salt fluxes due to evaporation, precipitation and sea-ice changes but not the FW addition term (the FW addition term is equivalent, at its maximum, to a salinity flux of 1.9×10^{-5} $kgm^{-2}s^{-1}$ south of 63°S). The areas of maximum Southern Ocean salt flux increase (Figure 1.5b) correspond well to the maximum sea-ice vol-

ume (height) increase in Figure 1.5a. The enhanced ice production is due to surface cooling which in turn is due to the suppresion of AABW overturn. This explains the more rapid return to AABW production in our study compared to Bi *et al.* (2001), who by warming the globe as a whole, warmed the global ocean and reduced sea-ice area, thus also reducing surface salt fluxes. Since in FW_{SO} this effect acts to increase AABW production after suppression by the FW anomaly, we can refer to it as a stabilising (or 'negative') feedback. The sea-ice feedback tends to work in the reverse, or 'positive' sense in the North Atlantic, where an increase in sea-ice suppresses surface ocean heat loss/evaporation, thereby reducing deep overturning (see for example Lohmann and Gerdes, 1998). In this positive feedback scenario, sea-ice acts to insulate the ocean from the colder overlying atmosphere, and thus unless there is sufficient sea-ice transport away from the formation areas (achieved by the westerly winds in the Southern Hemisphere), then sea-ice will inhibit the heat exchange necessary for cooling of surface waters, and thus overturning. Clearly the North Atlantic and Antarctic regions differ in this regard. Vertical diffusion could also be contributing to the removal of the surface FW anomaly and restoration of an unstable water column. The relevant timescale is $\tau = h^2/\kappa_v$ where h is the scale of stratification and κ_v the vertical diffusivity in the abyssal ocean. With $h = 10^3 m$ (Munk and Wunsch, 1998) and $O(\kappa_v) = 1.3 cm^2 s^{-1}$ in our model, $O(\tau) \approx 250 yrs$, which is slighly longer than the timescale of abyssal recovery seen in Figure 1.2 but nevertheless, this process could be playing a contributing role in the re-establishment of AABW sinking and abyssal overturning.

In summary, once FW forcing ceases in FW_{SO}, localised convection is re-established around Antarctica, aided by the perpetual upwelling of salty CDW combined with increased sea-ice and a reduced stratification arising from deep ocean warming. The convection brings more warm, saline water to the surface (see Figure 1.7a) which cools, sinks and continues the process of re-establishing a density structure similar to the control experiment. A large reason for the differing THC responses between the hemispheres is the different way in which salt is transported poleward, which in turn is due to different land-mass geometries. The process of suppressing AABW with FW does not suppress the oceanic salt transport or fluxes that normally maintain AABW production, quite unlike the classic Stommel (1961) climate response characteristic of the North Atlantic.

1.3.4. Climatic Effects

The reduction in sea surface (SST) and surface atmospheric (SAT) temperature in FW_{SO} at 150 years (Figure 1.4c & Figure 1.8a) is equivalent to a zonal average

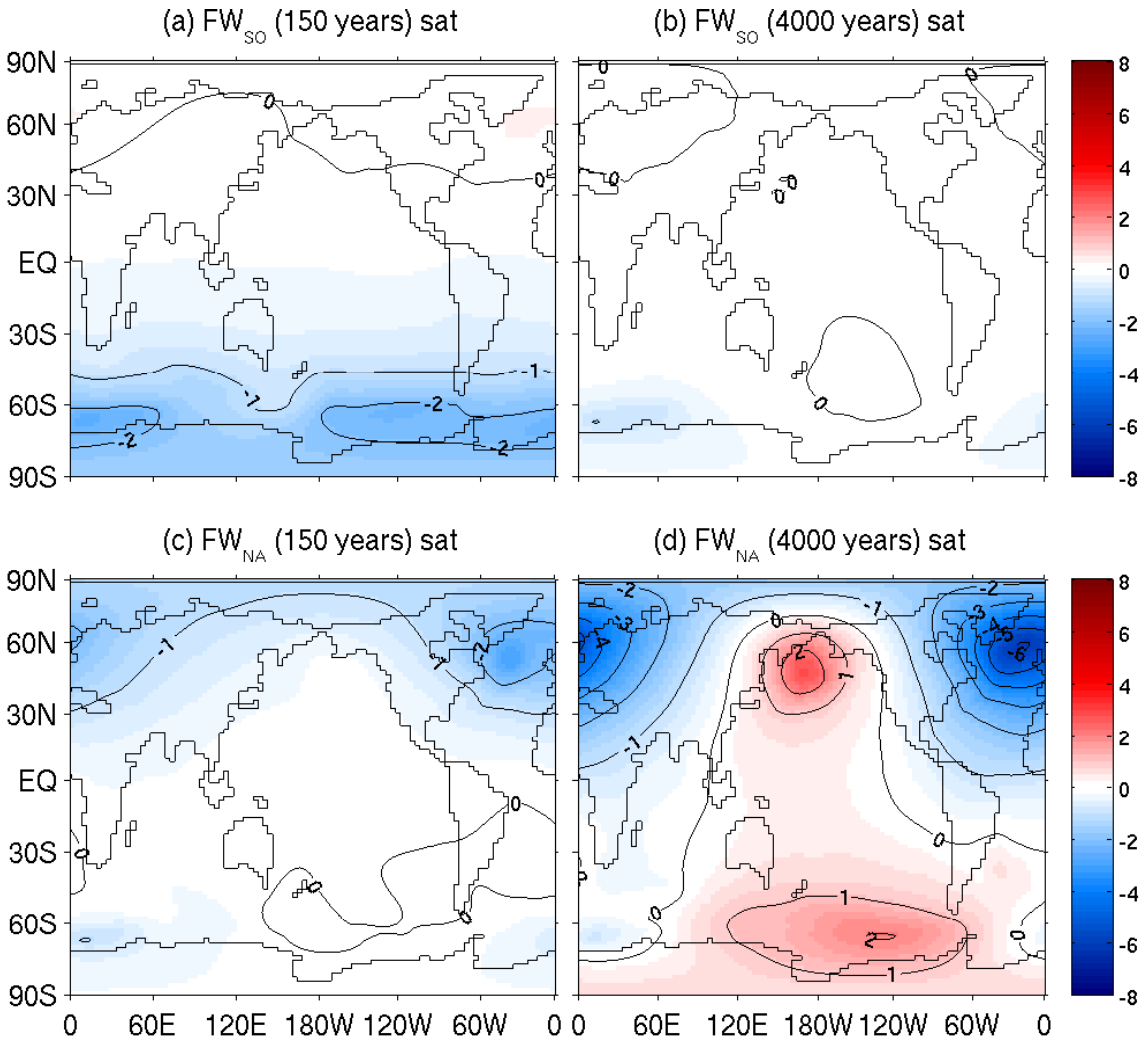

Figure 1.8. Difference fields (from CNTRL) of surface sea and surface air temperature for FW_{SO} and FW_{NA} at 150 years (left), and 4000 years (right). The data is taken from a 1 year average. Contour interval 1°C.

cooling south of 63° S of 0.2° C and 2.0° C, respectively. The maximum response in SAT is comparable to the corresponding year 150 zonal average cooling of SAT over the North Atlantic (2.1° C north of 51.3° N) in FW_{NA} (Figure 1.8c). However, due to the different long-term changes, the cooling over the North Atlantic increases to reach a steady-state value of 4.5° C, whilst the Southern Hemisphere SAT cooling is almost totally damped out within a few hundred years of the end of the FW pulse. The maximum zonal response in SST during FW_{SO} (at 150 years) of 0.2° C is much smaller than the 1.4° C seen over the North Atlantic in FW_{NA} at the same time (Figure 1.4d). Like SAT, this SST cooling over the North Atlantic during FW_{NA} increases during the course of the experiment, to reach a steady state value of 2.9° C by year 4000, whilst in FW_{SO}, it returns to within 0.05° C of CNTRL values a

few hundred years after the FW pulse ends.

The maximum surface atmospheric cooling over the Australian and New Zealand region in FW_{SO} is almost 1° C (Figure 1.8a), with the -2° C contour almost reaching the southern tip of South America at 150 years. The cooling over North America and Europe adjacent to the North Atlantic at the same time in FW_{NA} is of a similar order (Figure 1.8c). However, this cooling increases over the course of the experiment to reach more than 4° C over parts of Western Europe and eastern Canada (Figure 1.8d), whilst the Southern Hemisphere cooling in FW_{SO} is almost totally removed by 4000 years (Figure 1.8b). Remnant cooling remains only near the Antarctic coastline - and this persists at less than 1° C cooling - giving a zonal average cooling of just 0.3° C south of 63° S.

Even though in FW_{SO} the maximum surface ocean temperature reduction over the Southern Ocean is modest, the temporary suppression of convection suppresses the upwelling of warmer water during the FW pulse period, allowing the sea-ice volume to increase dramatically (Figure 1.5a). The sea-ice height over the major AABW formation regions of the Ross and Weddell Seas increases by up to 0.5 m, whilst the area coverage of sea-ice also increases over other regions; both effects increase the original sea-ice volume by more than 20 %. A greater ocean surface area covered by sea-ice leads to a reduction in heat fluxes from the ocean to the atmosphere, contributing significantly to the local cooling in atmospheric temperature. The sea-surface temperature only cools slightly, as the high latitude Southern Ocean is already close to freezing point. Once the ocean comes back into equilibrium with the surface air temperature, ocean temperatures return to within 0.05° C of CNTRL by 4000 years.

There is a 'see-saw' response in FW_{NA} in which the south Pacific SAT increases in temperature by more than 2° C, as less heat is transported into the North Atlantic, being eventually balanced by a heat gain in the south (Figure 1.8d). Thus a NADW 'shutdown' or weakening would possibly exacerbate the effects of global warming over this region of the Southern Hemisphere. In FW_{SO}, however, there is only a very weak inter-hemispheric response, with a slight temporary warming over the far North Atlantic (Figure 1.8a).

Lower evaporation over the slightly cooler and ice-covered high latitude Southern Ocean during AABW suppression results in a zonal average decrease in precipitation south of 63° S of around 10% (73 mm/year), which could also aid in capping surface

freshening (applied at the rate of 600 mm/year at the height of the pulse). During the peak FW addition, the ACC weakens by around 15 Sv (Figure not shown) due to the reduced meridional density gradient across the region.

1.3.5. Hysteresis Experiments

In the hysteresis experiments we apply the FW flux at the rate of 0.2 $Sv/1000\ years$ over the high latitude Southern Ocean (HYS_{SO}) and 0.08 $Sv/1000\ years$ over the North Atlantic (HYS_{NA}). The former is consistent with the North Atlantic hysteresis experiments carried out by Gregory *et al.* (2003). The initial HYS_{SO} experiment applied FW to the same limited area as the FW_{SO} experiments (south of 63° S). However, in that experiment, after AABW initially showed a steady decrease, it rapidly re-initiated. Since FW does not accumulate at the Antarctic continental margin, the rate of FW addition becomes important: surface and oceanic salt feedbacks in the Southern Ocean do not re-enforce the applied freshening - as occurs in North Atlantic hysteresis experiments - and thus the AABW response to FW additions depends on the rate of change of the FW addition rate, not just the FW addition rate itself. To carry out the hysteresis experiments then, the area of the FW addition was extended north to 60° S, maintaining the same local FW fluxes, but increasing the net volume of water added. For HYS_{SO} the linearly increasing FW flux was applied for 3500 years before symmetrically returning to zero (Figure 1.9b) at year 7000.

The hysteresis experiment HYS_{SO} results are shown in Figure 1.9a (blue solid curve). It should be noted that because of the dependence on the rate of change of FW addition rate, that these curves are not unique. However, they do illustrate the entirely different behaviour of AABW compared to the North Atlantic. Namely, because the feedbacks of the system do not re-enforce the perturbation, the response of the overturning is not smooth. AABW rapidly switches back 'on' in a series of steps a few hundred years after FW forcing reverses direction (at around 0.52 Sv). Though AABW seems to demonstrate two states for the same forcing at this time, these are not steady as is revealed by forward integration with FW forcing held constant (Figure not shown). AABW switches 'on' more quickly in the downward phase of the FW application. In these hysteresis experiments, with salt compensation over the world ocean outside of Antarctica (including the North Atlantic), NADW starts to decrease a few hundred years after the Southern Ocean FW flux has started to decrease (increase over the North Atlantic). To reduce this complicating feature of a reacting NADW water mass, an experiment with no salt compensation is also shown

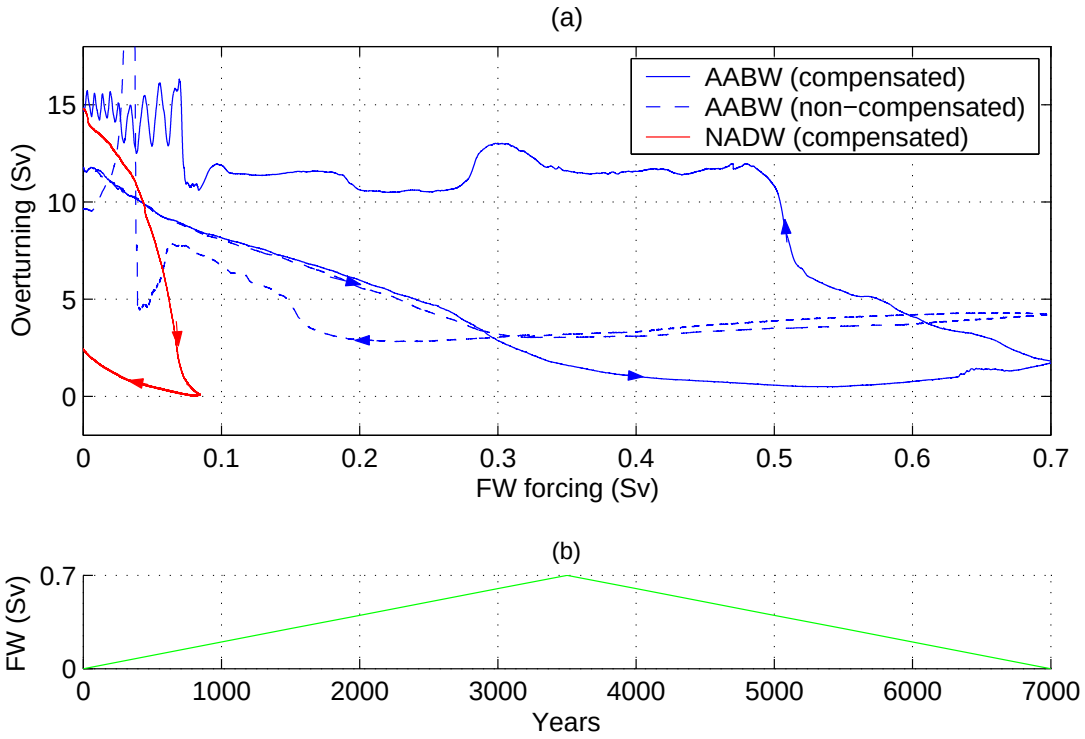

Figure 1.9. Overturning response to a slow FW forcing (0.2 Sv/1000 years for HYS_{SO}, and 0.08 Sv/1000 years for HYS_{NA}). (a) Overturning vs FW forcing. The trajectories show FW forcing increasing to the right, and decreasing going to the left. The North Atlantic overturning (blue line) can be considered to be in quasi-steady state at each point along the curve. The Southern Ocean overturning for different FW forcings is not in quasi-steady state: onward integration with forcing held constant does not maintain the same state. (b) The FW forcing versus time. Vertical scale is in Sverdrups (Sv).

(blue dashed line). AABW recovers along nearly the same path on reversal of the FW forcing, until a large oscillation occurs toward the end of the experiment. The oscillations seen in the last few centuries of these experiments are due to extremely reduced stratification in a much fresher ocean, making vigorous overturning more susceptible to surface heat and salinity flux changes.

1.4. Summary and Conclusions

We have demonstrated that the difference in response to FW perturbations of the North Atlantic and high latitude Southern Ocean arises from different thermal and salt feedbacks, caused by fundamental differences in land-mass geometries. In the North Atlantic, the dominant salt feedback is via surface water advection from

lower latitudes. If NADW slows, this salt advection also slows, and the natural feedbacks of the system enhance the applied perturbation (Figure 1.10). The presence of the Drake Passage gap blocks this feedback in the Southern Hemisphere, and it is instead the upwelling of saline CDW and northward Ekman transport of FW that transports salt into the high-latitude Southern Ocean (Figure 1.10). Critically, the upwelling of deep saline water and northward Ekman transport of FW is largely independent of the rate of AABW sinking. Thus, when bottom water sinking is suppressed, salt continues to accumulate below the surface FW lens. Eventually, once the surface waters cool and the FW lens is dispersed, AABW formation is readily re-established. The system was found to be incapable of maintaining FW anomalies at the high latitude Southern Ocean surface in the absence of sustained forcing. Sea-ice is affected by FW addition but in a stabilising sense; namely, on suppression of AABW there is surface cooling, growth of more sea-ice, and hence an increase in surface brine input. Combined with a deep ocean warming while AABW slows, these effects lead to gravitational instability and the restablishment of convection, bringing deep saline water to the surface, where the thin FW layer is further mixed away. Overturning is thus restarted soon after the FW perturbation has ceased.

The difference in North Atlantic and Antarctic salt feedbacks is due to (1) colder Antarctic waters which allow for extensive sea-ice formation once overturning is slowed; (2) differing continental geometries which allow wind-forced upwelling to dominate in the Southern Ocean, and (3) a different vertical ocean structure, with warm deep water underlying cold surface water in the high-latitude Southern Ocean. If we accept that the cooler temperatures around Antarctica are due, at least in part, to the thermal isolation caused by this differing continental geometry, and that the persistence of the wind-forced upwelling arises because of the Drake Passage Effect, then we conclude that the differing land-mass geometry is the fundamental reason for the difference in behaviour of NADW and AABW under identical FW perturbations.

It is interesting to note the remarkable steadiness of the high latitude Southern Ocean temperature over the course of FW_{SO} (maximum zonal mean change south of $63°S$ of $0.2°$ C from Section 1.3.4). Ocean temperatures in this region are kept so cold (near freezing point) by sub-zero katabatic winds blowing over the ocean, originating over the Antarctic land-ice mass. In the model, the effect of the Antarctic ice on maintaining cool SST is parameterised by way of meridional atmospheric

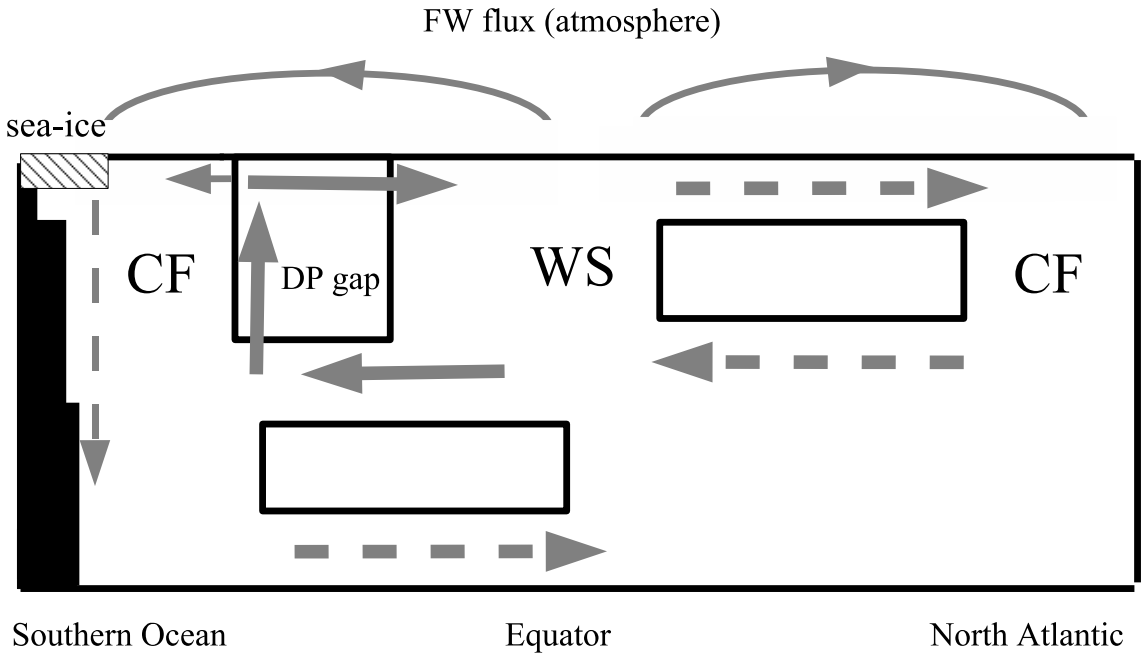

Figure 1.10. Schematic diagram highlighting the key salinity feedbacks in the high latitude Southern Oceans (left) and the North Atlantic (right), based on the simplified *Stommel1986* (1961) box model where sinking occurs in the high latitude basin in each case. WS denotes warm, saline, CF denotes cold, fresh and DP gap denotes Drake Passage. Arrows indicate salt transport mechanisms. A dashed line indicates the transport is dependent on the sinking (in either hemisphere). A solid line indicates that the transport is independent of sinking. In the NA, there is one positive (destabilising) feedback. In the high latitude Southern Ocean, there is one independent feedback (wind driven upwelling), and one stabilising feedback (sea-ice). Thermal feedbacks are not shown.

diffusion. This influence of the land-ice maintains colder surface temperatures than would otherwise be expected, even when the higher latitude regions of the AABW formation zones (compared to the North Atlantic) are taken into account. In fact, this thermal discrepancy between the Southern and Northern Hemisphere overturning regions leads to water densities in the polar Southern Ocean that are greater than any other water-mass in the global ocean. The large density difference between NADW and AABW (0.5 kgm^{-3}), combined with the deep Drake Passage sill, leads to AABW being highly stable to FW perturbations. This leaves AAIW and NADW as the main interactors in an interhemispheric see-saw of the ocean THC. If the Antarctic terrestrial ice sheet were absent, or the FW forcing persisted on timescales that allowed the ice sheet to adapt, then the surface water would be warmer, and the stability of AABW is likely to be reduced.

In conclusion, the response of AABW to FW perturbations is entirely different to NADW. In the North Atlantic, the freshening is enhanced by a positive salt advection feedback. In the Southern Ocean, the salt feedbacks are stabilising and combine to restart AABW after the FW addition ceases, regardless of the FW flux intensity or duration. This allows the thermal preference for Antarctic sinking to preclude a steady 'off' state for AABW in the model considered here. Although these experiments have been conducted using a simple atmospheric model rather than a 3-D dynamic AGCM, the stabilising feedbacks that have been highlighted are mainly limited to the ocean-ice system. In addition, all experiments have been re-run with a dynamic wind feedback included, and robust results were obtained. Hence, it is most likely that the feedbacks identified in this study would be present in full dynamic coupled climate system models.

Part II

Glacial climate experiments

Chapter 2

AABW and NADW stability, and the North Pacific

Abstract. Recent studies have shown North Atlantic Deep Water formation is highly sensitive to changes in the Southern Ocean. In a modern climate, positive heat or freshwater perturbations over the Southern Ocean can trigger an increase in North Atlantic Deep Water. In a glacial climate, positive heat perturbations over the Southern Ocean have a similar effect. These results are in agreement with a bipolar density see-saw operating between the hemispheres. By conducting freshwater sensitivity experiments, we find that the opposite is true for a glacial climate; namely a freshwater perturbation over the Southern Ocean can collapse North Atlantic Deep Water via a freshwater anomaly that propagates into the North Atlantic. Unlike the modern climate, the glacial climate is associated with a more fragile thermohaline circulation, whereby the negative effect of the surface salinity anomaly on North Atlantic Deep Water formation is able to dominate the bipolar density see-saw. Once North Atlantic Deep Water shuts down, North Pacific Intermediate Water increases from 2.1 Sv to 12.1 Sv, showing that the North Pacific/North Atlantic see-saw also operates in a glacial climate.

2.1. Introduction

Recent studies have shown the sensitivity of North Atlantic Deep Water (NADW) formation to perturbations of heat or freshwater (FW) over the Southern Ocean (Stouffer *et al.*, 2007; Weaver *et al.*, 2003; Trevena *et al.*, 2008; Knorr and Lohmann, 2003). Knorr and Lohmann (2003) showed that NADW could be triggered from the 'off' to the 'on' state by forcing a glacial to non-glacial transition in sea surface temperature (SST) over the Southern Ocean. Weaver *et al.* (2003) found that a NADW 'off' to 'on' transition can be triggered if an amount of FW roughly equivalent to meltwater pulse 1A (occurring 14.6 ka before present (BP) and raising global sea levels by 20m) is applied to the Southern Ocean. These results support the density see-saw hypothesis put forward by Bryan (1986), and later refined by Saenko *et al.* (2003), in which a density decrease in one hemisphere favours deep overturning in the other hemisphere. In the case of heating or freshening over the Southern Ocean, the density of the Southern Ocean decreases, Antarctic Intermediate Water (AAIW) production weakens, and NADW overturning is strengthened.

The above results suggest that the surface buoyancy changes in the Southern Ocean could have been responsible for triggering the last Northern Hemisphere deglaciation - via increased northward oceanic heat transport when NADW is switched 'on'. This idea relies on the assumption that NADW was collapsed in the glacial climate state. However, there is much evidence to suggest that NADW was only weakened rather than 'off' at the time of the Last Glacial Maximum (LGM), 21 ka BP (eg: Boyle and Keigwin, 1987; Meissner *et al.*, 2003; Lynch-Stieglitz *et al.*, 2007). An LGM climate with NADW 'on', albeit sluggish, is less able to account for the heating and de-glaciation of the Northern Hemisphere via the effects noted above. For example, if present-day NADW overturning is $21.6Sv$ and glacial NADW overturning is $13.7Sv$ (as in Montenegro *et al.*, 2007), then a transition from glacial to interglacial overturning requires an increase of just $7.9Sv$ - only a third of the $21.6Sv$ increase that would occur if the initial glacial overturning was zero.

Since overturning is strongly linked to northward oceanic heat transport, the increase in heat transport between the glacial and interglacial state is also much less in the case of an initial glacial state with weakened, instead of collapsed, NADW. This makes the choice of initial glacial climate state critical. For example, Weaver *et al.* (2003) started their experiments from a modern-day climate in which NADW was switched 'off' via a FW pulse applied over the North Atlantic. In reality, a glacial climate state will have globally cooler ocean temperatures, not just cooler temperatures over the North Atlantic. A cooler ocean is generally less sensitive to density changes arising from temperature fluctuations, due to the non-linearity of

the equation of state. Essentially density depends more on salinity than temperature at cooler conditions, so that in a glacial climate, NADW is likely to be less stable to FW perturbations. This decreased dependency on temperature in a colder climate was shown by de Boer *et al.* (2007) to result in weaker global overturning in a colder climate. To test the sensitivity of a glacial climate characterised by weak NADW formation to Southern Ocean FW input, we apply FW pulses to the Southern Ocean in both modern-day and glacial climates.

2.2. Model

We use the University of Victoria Intermediate Complexity Climate (UVic) model, (Weaver *et al.*, 2001). The ocean component has 19 depth levels, a resolution of 3.6 degrees longitude $\times$ 1.8 degrees latitude, and is coupled to a simple energy-moisture balance model of the atmosphere and a dynamic-thermodynamic model for sea-ice. The atmospheric model includes advection and diffusion of moisture and the sea-ice model includes prediction of the ice thickness and ice area fraction in each grid cell. The climate model is linked to prescribed land-ice that is static in time, but can be set to values between the present-day and 21 ka BP.

Enhanced wind-driven surface mixing is approximated using vertical diffusion coefficients of $1cm^2s^{-1}$ and $0.5cm^2s^{-1}$ in the top two layers. Vertical diffusion in the deeper layers varies according to the tidal mixing processes developed by Jayne and St. Laurent (2001), with greater vertical diffusivity around rough topography. A background diffusivity (K_b) of $0.15cm^2s^{-1}$ is used in addition to the tidal mixing distribution. The ocean model incorporates the Gent and McWilliams (1990) parameterisation of eddy advection effects, and a rigid-lid approximation is used. Insolation and CO_2 are prescribed for each experiment, whereas air and ocean temperature, and ocean salinity, are allowed to evolve freely. Wind is fixed within an annual cycle based on the monthly fields from the NCEP/NCAR reanalysis over the period 1958-1997. From both the modern-day and LGM simulations, we apply FW to the region south of $63°S$, equivalent to a $25m$ global sea level rise over 500 years (experiments $CNTRL_{FW}$ and LGM_{FW}, respectively). Experiments with smaller FW pulses, equivalent to global sea level rise of $20m$, produced similar results.

2.2.1. Modern Day Simulation

The modern-day CNTRL experiment is forced with pre-industrial insolation and CO_2 (280 ppm), and pre-industrial land-ice. The equilibrium control state generates approximately $17.6Sv$ of NADW (Figure 2.2b), which lies between the $12.8Sv$ obtained by Simmons *et al.* (2003) with $K_b = 0.1cm^2s^{-1}$ and the $21.6Sv$ obtained by

Montenegro *et al.* (2007) with $K_b = 0.2cm^2s^{-1}$. North Pacific Intermediate Water (NPIW) is weak ($1.3Sv$) and shallow ($< 500m$; Figure 2.2a), being the result of localised convection of mode waters. Formation of AABW is characterised by a cell of strength $3.6Sv$ (not shown), corresponding to overturning adjacent to Antarctica. Another measure of the model's AABW strength, which depends less on zonal aliasing, is the net northward flow of bottom water in the abyssal cell centred near $40°S$. This cell has strength $11.7Sv$ in CNTRL.

2.2.2. LGM Simulation

For the glacial LGM experiment, land-ice is prescribed to values estimated for 21 ka BP (based on the ice-4g re-construction of Peltier, 1994). Orbital configurations are also set to 21 ka BP, and CO_2 is set to 200 ppm. The resulting glacial climate state has a global mean SST and SAT cooling relative to CNTRL of $2.0°C$ and $3.1°C$ respectively. Global SST differences between experiments LGM and CNTRL are shown in Figure 2.1. Maximum SST cooling of over $5.0°C$ is seen in the North Atlantic north of $45°N$, consistent with PMIP2 simulations (Bracannot *et al.*, 2007). NADW formation weakens to $14.3Sv$ (Figure 2.2d, a net reduction of 23 percent) and the formation areas also shift slightly southward, particularly the sinking at $60°N$ (Figure 2.2d). NPIW strengthens slightly to $2.1Sv$ (Figure 2.2c). AABW sinking decreases from $3.6Sv$ to $2.7Sv$, whilst the abyssal cell barely changes, exhibiting an equilibrium value of $11.6Sv$.

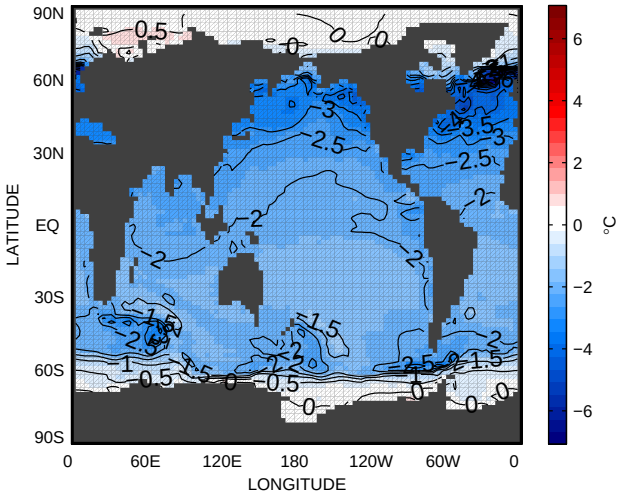

Figure 2.1. Simulated sea surface temperature (SST) difference from CNTRL for the LGM simulation. Values are based on a 1-year average. Contour interval is $0.5°C$.

2.3. Results

During the first 100 years of the LGM_{FW} experiment, NADW increases from $14.3Sv$ to $17.4Sv$ (Figure 2.3a). Over the same period in $CNTRL_{FW}$, the response is similar, with NADW increasing from $17.6Sv$ to $20.5Sv$. This increase is due to the density see-saw effect (Saenko *et al.*, 2003), whereby freshening the AAIW formation regions in the Southern Ocean leads to a decrease in local density, an increase in the density contrast between the Southern Ocean and the North Atlantic, thereby increasing overturning in the North Atlantic.

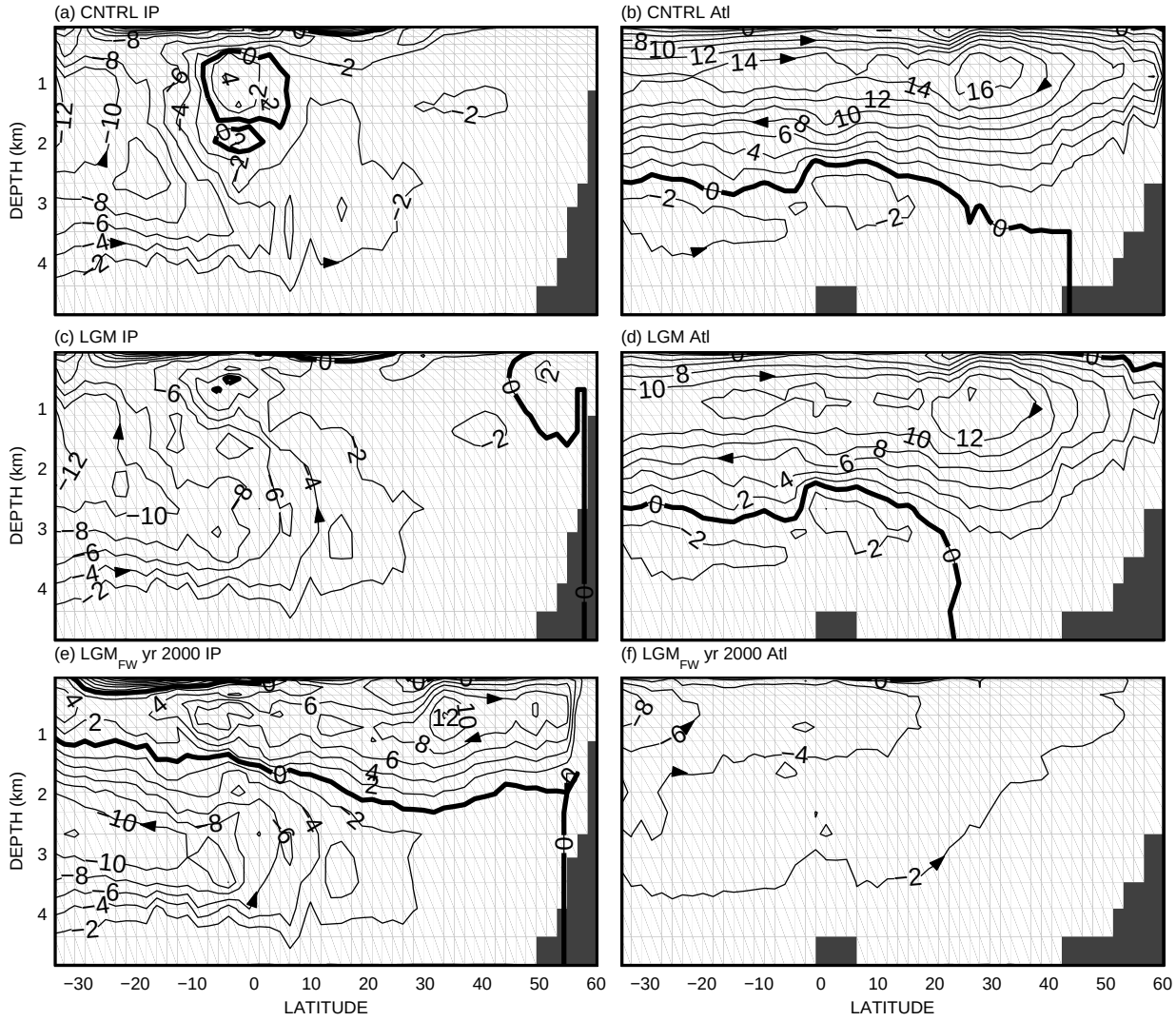

Figure 2.2. Meridional overturning streamfunctions for the Indo-Pacific (left column) and Atlantic (right column) for steady-state CNTRL (top row), and LGM (middle row); and for year 2000 LGM_{FW} (bottom row). Values based on a 1-year average. Contour interval is $2Sv$. ($1Sv = 1 \times 10^6 m^3 s^{-1}$)

After this initial period, the glacial climate responds very differently. In LGM_{FW}, NADW steadily decreases, attaining a value of zero by 1000 years, where it remains stable. The Atlantic meridional streamfunction at 2000 years (Figure 2.2f) confirms the lack of NADW formation in the final state of this experiment. By contrast, in $CNTRL_{FW}$, NADW initially decreases to $14.4Sv$ at around 540 years, but then it increases back to just over $20Sv$ by year 1000, before decreasing smoothly to a new steady-state by year 2000, where NADW is overturning at the rate of $18.8Sv$.

Original In both cases above, the NADW decrease after the initial increase is due to the Southern Ocean freshwater anomaly being transported northwards of the Antarctic Circumpolar Current (ACC) via Ekman transport (Stouffer *et al.*, 2007; Trevena *et al.*, 2008). This FW then intrudes into the North Atlantic via the Benguela Current and the Gulf Stream. Figures 2.4a, b show a similar negative sea surface salinity (SSS) anomaly in the Atlantic at year 100 of both $CNTRL_{FW}$ and LGM_{FW}. Yet despite this similarity, there is a very different response in the North Atlantic. In the modern-day climate the extra FW in the surface layers of the North Atlantic does not induce a collapse of NADW; yet in the glacial climate NADW shuts down (Figure 2.3a). The reason for this is the density contrast between AAIW and

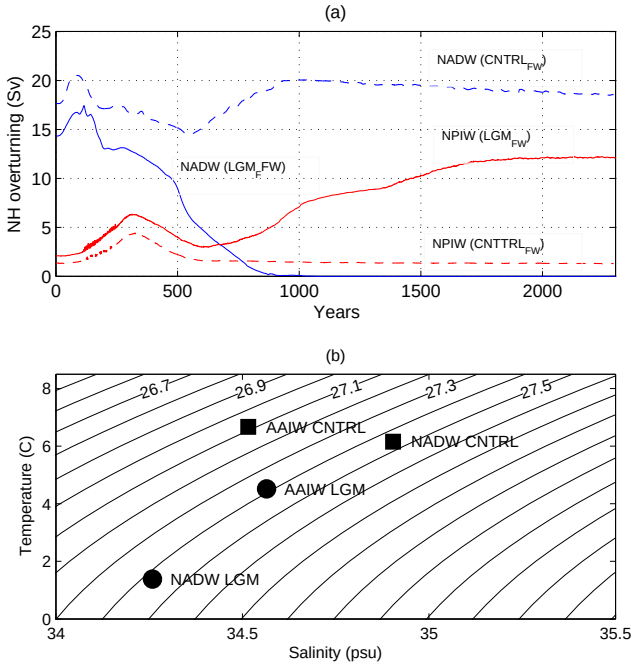

Figure 2.3. (a) Overturning time-series for North Atlantic (blue) and North Pacific (red) in the LGM_{FW} (solid lines) and $CNTRL_{FW}$ (dashed lines) experiments. (b) Temperature-Salinity (T-S) plot showing surface density of NADW and AAIW formation regions in the CNTRL state (squares) and LGM state (circles).

NADW in the unperturbed states (Figure 2.3b).

New In both cases above, the NADW decrease after the initial increase is due to the Southern Ocean freshwater anomaly being transported northwards of the Antarctic Circumpolar Current (ACC) via Ekman transport (Stouffer *et al.*, 2007; Trevena *et al.*, 2008). This FW then intrudes into the North Atlantic via the Benguela Current, shallow cross equatorial flow and then the northern limb of the North Atlantic tropical gyre or Gulf Stream. Once a FW anomaly is present in this region, the well known positive salt feedbacks operating in the North Atlantic act to amplify the initial anomaly and lead to a shut-down - that initially occurs more gradually than when the FW anomaly is applied immediately to the NA region as in FW_{NA} in Part I. The initially slower response of NADW to the FW anomaly in LGM_{SO} could also be related to the increase vertical diffusive timescale, h^2/κ_v, associated with the reduced diffusion in the tidal mixing scheme used in LGM_{SO}.

Figures 2.4a, b show a similar negative sea surface salinity (SSS) anomaly in the Atlantic at year 100 of both $CNTRL_{FW}$ and LGM_{FW}. Yet despite this similarity, there is a very different response in the North Atlantic. In the modern-day climate the extra FW in the surface layers of the North Atlantic does not induce a collapse of NADW; yet in the glacial climate NADW shuts down (Figure 2.3a). The reason for this is the density contrast between AAIW and NADW in the unperturbed states (Figure 2.3b).

Compared to CNTRL, LGM has a thicker annual mean sea-ice coverage over the North Atlantic, and sea-ice also extends further to the south (Figure not shown). This insulates the ocean from the atmosphere, reducing air-sea heat fluxes that promote North Atlantic overturning (Lohmann and Gerdes, 1998). The overturning thus weakens and shifts south. The reduced overturning results in less northward salt transport into the North Atlantic, with surface waters $0.7psu$ fresher compared to CNTRL (Figure 2.3b). The effect on density of this fresher water is offset by the fact that the LGM waters of the North Atlantic are $5°C$ colder. Thus, despite very different temperature-salinity (T-S) signatures, the water density over NADW formation regions is very similar between LGM and CNTRL (Figure 2.3b). By contrast, over AAIW formation regions, surface density is $\approx 0.3kgm^{-3}$ greater in LGM than CNTRL due to $\approx 2°C$ cooler surface waters (Figure 2.3b). The bipolar density see-saw is thus sitting much closer to its tipping point in LGM, and is more sensitive to the FW anomaly that propagates into the North Atlantic after a few hundred years. In addition, the increased dependency of density on salinity in the colder LGM climate means that the FW anomaly induces a greater increase in surface buoyancy (by 0.1 kgm^{-3}), and thus also surface stratification, in the LGM case.

The initial increase of NADW in LGM_{FW} causes a regional SAT warming of $\approx 0.5°C$ over the North Atlantic (Figure 2.4c). The Southern Ocean cools during this time, in agreement with the results of Weaver *et al.* (2003). Once NADW decreases to zero however, regional SAT cools by over $3.5°C$ in the North Atlantic, similar to the difference between a NADW 'on' and 'off' state in the modern-day climate (Weaver *et al.*, 2003). In contrast, the differences in global SAT in the CNTRL climate are minimal (not shown), since the experiment returns to close to its initial state by 2000 years in $CNTRL_{FW}$ (Figure 2.3a).

While NADW decreases, NPIW deepens and increases to $12.2Sv$ by year 1800, whereupon it remains stable, thus becoming North Pacific Deep Water (NPDW;

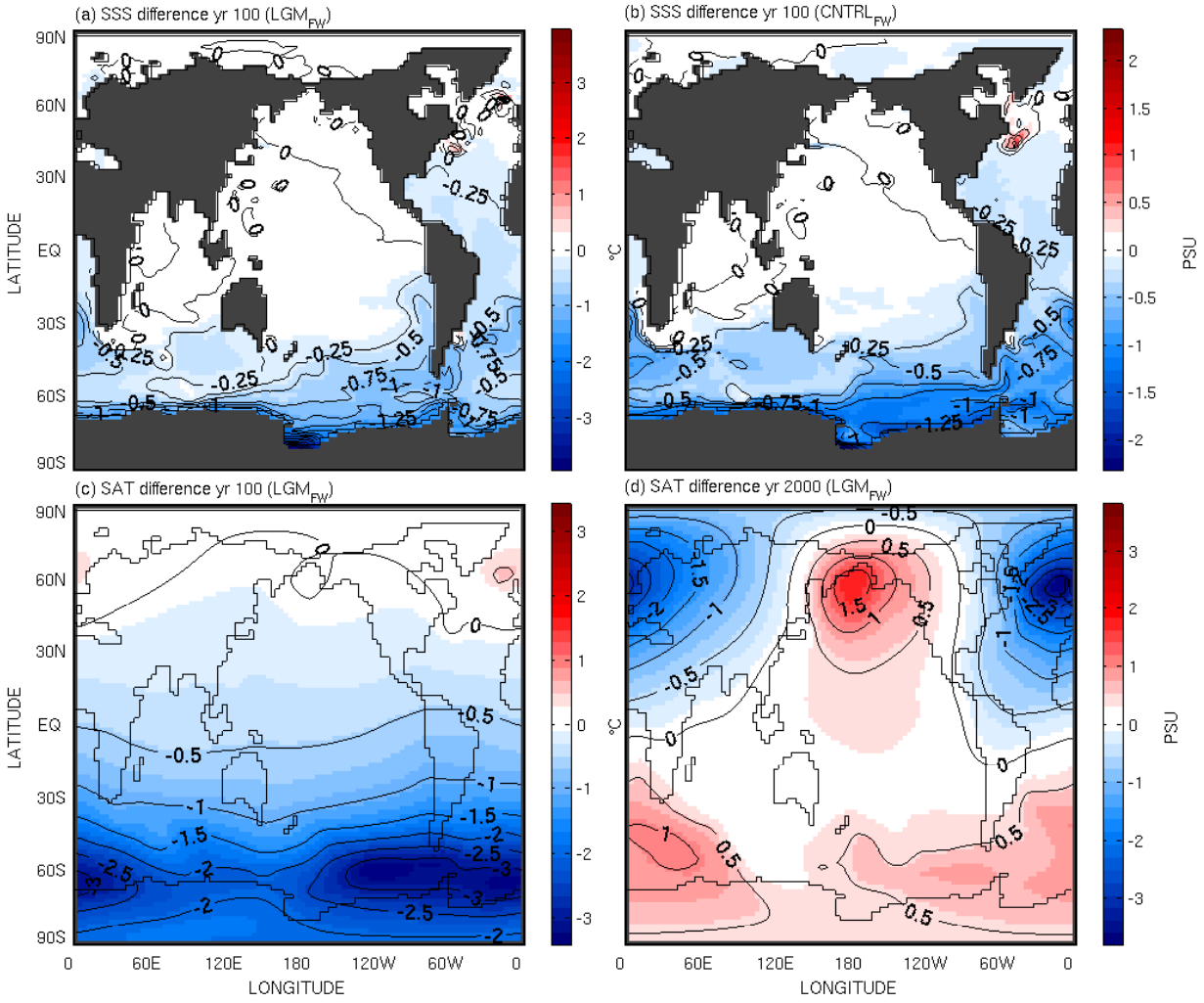

Figure 2.4. Changes in sea surface salinity (SSS) (top row) for (a) LGM_{FW} and (b) $CNTRL_{FW}$ after 100 years. Surface air temperature (SAT) (bottom row) for the LGM_{FW} experiment at (c) 100 years and (d) 2000 years. All values are based on a 1-year average. Contour intervals are 0.25 psu and $1°C$ respectively.

Figure 2.2e, 2.3). This is due to the North Pacific/North Atlantic sea-saw (Saenko *et al.*, 2004; Kiefer *et al.*, 2001) in which the Stommel (1961) inter-hemispheric salinity feedbacks are also seen to operate between different ocean basins. In particular, a freshening in the Atlantic basin causes more high salinity water to accumulate in the North Pacific, where it increases overturning. This strengthened overturning then increases northward heat and salt transport over the Pacific, increasing T-S over the North Pacific, and further re-enforcing the initial change that produced it. This see-saw effect can thus be seen to operate in a glacial climate, as well as the modern-day climate, in our study. The increase of NPDW formation causes SAT over the North Pacific to increase by over $1.5°C$ by 1400 years, where it remains steady (Figure 2.4d).

2.4. Summary and Conclusions

These results suggest that Southern Hemisphere meltwater pulses could have triggered a NADW shut down in past glacial climate states. Although we apply the FW uniformly around Antarctica instead of at specific locations of land-ice/glacial melt, the ACC ensures that surface waters at high latitudes of the Southern Ocean are reasonably well mixed over century time-scales. Such meltwater pulses in the Northern Hemisphere, and subsequent NADW shut down, are often invoked to explain cold Heinrich events, such as the Younger Dryas of 13 - 11.5 ka BP. Our results show that these cold periods could also be triggered by meltwater events in the Southern Hemisphere.

The result of NPIW increasing in depth and strength; and becoming NPDW is also interesting from the point of view of the paleo-climate record. Ohkouchi *et al.* (2002) found that Cadmium levels during the de-glaciation 15 ka BP in the North Pacific were almost the same as in the modern-day North Atlantic. They postulate that this could have been due to a convection cell in the northwest Pacific. Our simulations show that such NPDW could have arisen from a meltwater pulse in the Southern Ocean during the de-glaciation around 15 ka BP. Minoshima *et al.* (2007) argue such an increase in North Pacific ventilation was temporary; though in our simulation, the NADW 'off' state and concurrent NPDW 'on' state remain stable. However, we fix land-ice and orbital parameters. Reconstructions show the western Laurentide ice sheet adjacent to the Pacific mostly disappeared between 15 ka and 12 ka BP (Peltier, 1994). The melting of this ice sheet and subsequent FW pumped into the NP could have shut down NPDW, supporting the findings of Minoshima *et al.* (2007). Under this scenario, NADW would then re-initiate to modern-day values due to the NP/NA see-saw effect.

A Younger Dryas (YD) in which NADW is collapsed and an LGM in which NADW is on, seem to contradict the similar GRIP (EPICA, 2006) temperature records of these two periods. An active NADW has higher Atlantic northward oceanic heat transport, and hence should promote warmer SAT over the North Atlantic region. However, this is not necessarily true. Surface air temperature is also strongly affected by ice sheets; fore example, Bracannot *et al.* (2007) show that ice sheets and snow contribute to more than half the cooling over the Northern Hemisphere during the LGM. The LGM had more widespread and thicker ice sheets than those seen during the YD (Peltier, 1994). Hence, it is possible the LGM, with its larger ice sheets but with northward heat transport from sluggish NADW, could have a similar SAT signal over Greenland as the YD period with smaller ice sheets but collapsed NADW. The variation of NADW could still be expected to have a large effect on regional SAT when land-ice sheets remained fairly constant.

Since ice-sheets amplify climate signals, models with interactive land-ice are required to more fully explain the mechanisms leading to glacial-interglacial transitions. However, models without this feature can still provide insight into the way a colder climate with large land-ice sheets influences global ocean circulation responses to FW anomalies. These responses can then be evaluated against ice-sheet effects in more fully coupled models. Using an intermediate complexity model with static land-ice, we have shown that ocean circulation changes in response to FW anomalies over the Southern Ocean are very different in glacial and non-glacial climate states.

Chapter 3

Conclusions

Repeated and varied observations show Antarctica is losing mass (Chen *et al.*, 2009; Velicogna and Wahr, 2006; Zwalley *et al.*, 2005; Davis *et al.*, 2005; Ramillien *et al.*, 2006; Rignot *et al.*, 2008) and this could accelerate with climate change and warming oceans (Shepherd *et al.*, 2004; Thomas, 1979), though there are large uncertainties associated with the response of ice sheets to climate change - Allison *et al.* (2009) notes *"the largest unknown in projections of sea level rise over the next century is the potential for rapid dynamic collapse of ice sheets."* Precipitation records over the Southern Ocean are sparse, but reanalyses and modeling studies show a robust link between the Southern Annular Mode (SAM) and precipitation (Boer *et al.*, 2001; Cai and Watterson, 2002; Silvestri and Vera, 2003); with increases over high-latitudes and decreases over mid-latitutes. associated with a robust positive trend in the SAM since the $1960's$ (Thompson and Wallace, 2000; Marshall, 2003). Predicted precipitation changes over the Southern Ocean by the end of the $21st$ century from the IPCC AR4 report show increases of up to $\approx 150mm/year$ compared to the $20th$ century. The combined effect of all these sources of freshwater would be a freshening of the high latitude Southern Ocean and such freshening has been noted in observations (Bindoff and McDougall, 2000; Curry and Yashayaev, 2003; Rintoul, 2007). This freshening increases the stratification of the surface ocean, making it more stable, and causing changes in the deep Southern Ocean thermohaline circulation, AABW, noted by (Rintoul, 2007) and predicted by IPCC model projections (Sen Gupta *et al.*, 2008).

This thesis aimed to conduct a modeling study to examine the sensitivity of AABW to such increases in FW forcing over the Southern Ocean, and to investigate the role of the Southern Hemisphere thermohaline circulation as a whole (including AABW and AAIW) in the entire global thermohaline circulation system. The use of an Intermediate Complexity Coupled Climate Model (the UVic model) allowed a large

number of experiments on centennial to millenial timescales to be carried out. Experiments showed that:

* though AABW is stable to FW forcing on time-scales ranging from a few years to multi-millenial, the transient impacts of that forcing do include a drastic slowdown of AABW, an invigoration of NADW, and a Southern Hemisphere surface cooling signal that propagates well north, to the southern mid-latitudes and tropics.

* that the stability of this system changes markedly in a colder, glacial type climate due to changes in the stratification and hence stability of the ocean. This change in stability leads to the Southern Ocean becoming a vital part of the global THC in the glacial climate - acting as a trigger region for northern hemisphere overturning in both the North Atlantic and North Pacific.

An obvious extension of this study would be to conduct similar experiments in a fully coupled model so atmospheric responses and ocean-atmospheric feedbacks could be assessed; a clear limitation of this study being the simplistic nature of the energy-moisture balance single layer atmosphere in the UVic model. This study has been nearly completed, using the CSIRO Mk3L fully coupled climate model (Gordon *et al.*, 2002; Phipps *et al.*, 2011), and is in the process of being written up for review. It sheds further light on processes at play between the high latitude Southern Hemisphere and tropics, which could be of relevance to the real climate in the future centuries.

Bibliography

Allison, I., R. B. Alley, H. A. Fricker, R. H. Thomas and R. C. Warner, 2009: Review Ice sheet mass balance and sea level. *Antarctic Science*, doi:10.1017/S0954102009990 137. 1–14.

Aoki, S., M. Yoritaka and A. Masuyame, 2003: Multidecadal warming of subsurface temperature in the Indian sector of the Southern Ocean. *Journal of Geophysical Research*, **108**, doi:10.1029/2000JC000 307.

Bates, M. L., M. H. England and W. P. Sijp, 2005: On The multi-century Southern Hemisphere response to changes in atmospherice CO_2 concentration in a global climate model. *Met. Atmos. Physics*, **89**, 17–36.

Bentley, C. R., R. H. Thomas and I. Velicogna, 2007: Ice sheets. *Global Outlook for ice and snow. Nairobi: United nations Environment Programme*, 99–113.

Bi, D., W. F. Budd, A. C. Hirst and X. Wu, 2001: Collapse and reorganisation of the Southern Ocean overturning under global warming in a coupled model. *Geophysical Research Letters*, **28**, 3927–3930.

Bindoff, N. L. and J. McDougall, Trevor, 2000: Decadal Changes along an Indian Ocean Section at 32°S and Their Interpretation. *Journal of Physical Oceanography*, **30**, 1207–1222.

Bitz, C. M. and W. H. Lidcombe, 1999: An energy-conserving model of sea-ice. *Journal of Geophysical Research*, **104**, 15 669–15 677.

Boer, G. J., S. Fourest and B. Yu, 2001: The signature of the annular modes in the moisture budget. *Journal of Climate*, **14**, 3655–3665.

Bond, G., W. Broecker, S. Johnsen, J. McManus, L. Laberyie, J. Jouzel and G. Bonani, 1993: Correlations between climate records from North Atlantic sediments and Greenland ice. *Nature*, **365**, 143–147.

Boyle, E. A. and L. D. Keigwin, 1987: North Atlantic thermohaline circulation during the past 20,000 years linked to high-latitude surface temperature. *Nature*, **330**, 35–40.

Bracannot, P., B. Otto-Bliesner, S. Harrison, S. Joussaume, J.-Y. Peterchmitt, A. Abe-Ouchi, M. Crucifix, E. Driesschaert, T. Fichefet, C. D. Hewitt, M. Kageyama, A. Kitoh, A. Laine, M.-F. Loutre, O. Marti, U. Merkel, G. Ramstein, P. Valdes, S. L. Weber, Y. Yu and Y. Zhao, 2007: Results of PMIP2 coupled

simulations of the Mid-Holocene and Last Glacial Maximum - part 2: feedbacks with emphasis on the location of the ITCZ and mid- and high latitudes heat budget. *Climate of the Past*, **3**, 279–296.

Brix, H. and R. Gerdes, 2003: North Atlantic Deep Water and Antarctic Bottom Water: Their interaction and influence on the variability of the global ocean circulation. *Journal of Geophysical Research*, **108**, 4–1–4–17.

Bryan, F., 1986: High-latitude salinity effects and interhemispheric thermohaline circulations. *Nature*, **323**, 301–304.

Bryan, K. and L. J. Lewis, 1979: A water mass model of the world ocean. *Journal of Geophysical Research*, **84**, 2503–2517.

Cai, W. and I. G. Watterson, 2002: Modes of interanual variability of the Southern Hemisphere circulation stimulated by the CSIRO climate model. *Journal of Climate*, **15**, 1159–1174.

Chen, J. L., C. R. Wilson, D. Blankenship and B. D. Tapley, 2009: Accelerated Antarctic ice loss from satellite gravity measurements. *Nature Geoscience*, **2**, doi:10.1038/NGE0694. 859–862.

Clark, P. U., 2002: The role of the thermohline circulation in abrupt climate change. *Nature*, **22**, 301–304.

Clark, P. U., N. G. Pistas, T. F. Stocker and A. J. Weaver, 2002: The role of the thermohaline circulation in abrupt climate change. *Nature*, **415**, 863–869.

Curry, B., R. Dickson and I. Yashayaev, 2003: Change in the freshwater balance of the Atlantic Ocean over the past four decades. *Nature*, **426**, 826–829.

Davis, C. H., Y. Li, J. R. McConnell, M. M. Frey and E. Hanna, 2005: Snowfall-driven growth in East Antarctic ice sheet mitigates recent sea level rise. *Science*, **308**, 1989–1901.

de Boer, A., D. M. Sigman, J. R. Toggweiler and J. L. Russell, 2007: The effect of global ocean temperature change on deep ocean ventilation. *Paleooceanography*, **22**, PA2210.

De Conto, R. M. and D. Pollard, 2003: Rapid Cenozoic glaciation of Antarctica induced by declining atmospheric CO_2. *Letters to Nature*, **421**, 245–249.

Duffy, P. B. and K. Caldeira, 1997: Sensitivity of simulated salinity in a three dimensional ocean model to upper-ocean transport of salt from sea-ice formation. *Geophysical Research Letters*, **24**, 1323–1326.

EPICA, 2006: One-to-one coupling of glacial climate variability in Greenland and Antarctica. *Nature*, **444**, doi:10.1038/nature05 301.

Fairbanks, R. G., 1989: A 17,000-year glacio-eustatic sea level record: influence of glacial melting rates on the Younger Dryas event and deep-ocean circulation. *Nature*, **342**, 637–642.

Gehrels, R., 2010: Sea-level changes since the Last Glacial Maximum: an appraisal of the IPCC Fourth Assessment Report. *Journal of Quaternary Science*, **25**, DOI: 10.1002/jqs.1273. 26–38.

Gent, P. R. and J. C. McWilliams, 1990: Isoypycnal mixing in ocean general circulation models. *Journal of Physical Oceanography*, **20**, 150–155.

Gill, A. E., 1982: *Atmosphere-ocean dynamics*. New York: Academic Press, ISBN 0122835204, New York.

Goodman, J., Paul, 1998: The Role of North Atlantic Deep Water Formation in an OGCM's Ventilation and Thermohaline Circulation. *Climate Dynamics*, **28**, 1759–1785.

Gordon, H. B., R. J. L., M. R. McGregor, E. A. Dix, S. P. Kowalczyk, L. J. O'Farrell, L. J. Waterman, A. C. Hirst, S. G. Wilson, M. A. Collier, I. G. Watterson and T. I. Elliot, 2002: The CSIRO Mk3 Climate System Model. *CSIRO Technical Report No. 60*, ISBN 0 643 06878 3. 134 pages.

Gregory, J. M., O. A. Saenko and A. J. Weaver, 2003: The role of the Atlantic freshwater balance in the hyteresis of the meridional overturning circulation. *Climate Dynamics*, **21**, 707–717.

Griffies, S. M., A. Biastoch, C. Boning, F. Bryan, G. Danabasoglu, E. P. Chassignet, M. H. England, R. Gerdes, H. Haak, R. W. Hallberg, W. Hazeleger, J. Jungclaus, W. G. Large, G. Madec, A. Pirani, B. L. Samuels, M. Scheinert, A. S. Gupta, C. A. Severijns, H. L. Simmons, A. M. Treguier, M. Winton, S. Yeager and J. Yin, 2009: Coordinated Ocean-ice Reference Experiments (COREs). *Ocean Modelling*, **26**, 1–46.

Jacobs, S. S., C. F. Giulivi and P. A. Mele, 2002: Freshening of the Ross Sea During the Late 20th Century. *Science*, **297**, doi: 10.1126/science.1069 574 386–388.

Jayne, S. R. and L. C. St. Laurent, 2001: Parameterising tidal dissipation over rough topography. *Geophysical Research Letters*, **28**, 811–814.

Jouzel, J., V. Masson-Delmotte, O. Cattani, G. Dreyfus, S. Falourd, G. Hoffmann, B. Minster, J. Nouet, J. M. Barnola, J. Chappellaz, H. Fischer, J. C. Gallet, S. Johnsen, M. Leuenberger, L. Loulergue, D. Luethi, H. Oerter, F. Parrenin, G. Raisbeck, D. Raynaud, A. Schilt, J. Schwander, E. Selmo, R. Souchez, R. Spahni, B. Stauffer, J. P. Steffensen, B. Stenni, T. F. Stocker, J. L. Tison, M. Werner and E. W. Wolff, 2007: Orbital and millenial Antarctic climate variability over the past 800,000 years. *Science*, **317**, 793–796.

Kalnay, E., R. M. Kanamitsu, W. Kistler, D. Collins, L. Deaven, M. Gandin, S. Iredell, G. Saha, J. White, Y. Woollen, A. Zhu, Leetmaa and R. Reynolds., 1996: The NCEP/NCAR 40-year re-analysis project. *Bull. Amer. Meteor. Soc.*, **77**, 437–471.

Katz, M. E., K. G. Miller, J. D. Wright, B. S. Wade, J. V. Browning, B. S. Cramer and Y. Rosenthal, 2008: Stepwise transition from the Eocene greenhouse to the Oligocene icehouse. *Nature Geoscience*, **1**, 329–334.

Keeling, R. F. and B. B. Stephens, 2001: Antarctic sea-ice and the control of Pleistocene climate instability. *Paleooceanography*, **16**, 112–130.

Keffer, T. and G. Holloway, 1988: Estimating Southern Ocean eddy flux of heat and salt from satellite altimetry. *Letters to Nature*, **332**, 624–626.

Kiefer, T., M. Sarnthein, H. Erlenkeuser, P. M. Grootes and A. P. Roberts, 2001: North Pacific response to millenial-scale changes in ocean circulation over the last 60 kyr. *Paleooceanography*, **16**, 179–189.

Knorr, G. and G. Lohmann, 2003: Southern Ocean origin for the resumption of atlantic thermohaline circulation during deglaciation. *Nature*, **424**, 532–536.

Lee, M., J. Nurser, A, A. C. Coward and B. A. de Cuevas, 2006: Advective and Diffusive Transports of Heat and Salt in the Southern Ocean. *Journal of Physical Oceanography*, **37**, 1376–1393.

Levitus, S., R. Burgett and T. P. Boyer, 1994: *World Ocean Atlas (1994). Vol. 3 and 4 : Salinity and Temperature*. National Oceanic and Atmospheric Administration, U.S. Department of Commerce, Washington, D.C.

Lohmann, G. and R. Gerdes, 1998: Sea Ice Effects on the Sensitivity of the Thermohaline Circulation. *Journal of Climate*, **11**, 2789–2803.

Lynch-Stieglitz, J., J. F. Adkins, W. B. Curry, T. Dokken, I. R. Hall, J. C. Herguera, J. J.-M. Hirschi, E. V. Ivanova, C. Kissel, O. Marchal, T. M. Marchitto, I. N. McCave, J. F. McManus, S. Mulitza, U. Ninnemann, F. Peeters, E. F. Yu and R. Zahn, 2007: Atlantic Meridional Overturning circulation during the Last Glacial Maximum. *Science*, **1316**, doi: 10.1029/2002PA000 762.

Manabe, S. and R. J. Stouffer, 1988a: Two stable equilibria of a coupled ocean-atmosphere model. *Journal of Climate*, **1**, 841–866.

Manabe, S. and R. J. Stouffer, 1988b: Two stable equilibria of a coupled ocean-atmosphere model. *Journal of Climate*, **1**, 841–866.

Marshall, G. J., 2003: Trends in the Southern Annular Mode from observations and reanalyses. *Journal of Climate*, **16**, 4134–4143.

Meissner, K. J., A. Schmittner, A. J. Weaver and J. F. Adkins, 2003: Ventilation of the North Atlantic ocean during the Last Glacial Maximum: A comparison between simulated and observed radiocarbon ages. *Paleoceanography*, **18**, doi: 10.1029/2002PA000 762.

Miller, K. G., M. A. Kominz, J. V. Browning, J. D. Wright, G. S. Mountain, M. E. Katz, P. J. Sugarman, B. S. Cramer, N. Christie-Blick and S. F. Pekar, 2005: The Phanerozoic Record of Global Sea-Level Change. *Science*, **310**, 1293–1298.

Minoshima, K., H. Kawahata, T. Irino, K. Ikehara, K. Aoki, M. Uchida, M. Yoneda and Y. Shibata, 2007: Deep water ventilation in the northwestern north Pacific during the last deglaciation and the early Holocene (15-5 cal. kyr B.P. based on AMS $^{14}Cdating.Nucl.Instr.andMeth.inPhys.Res.B.$, **259**, 448 − −452.

Montenegro, A., M. Eby, A. J. Weaver and S. R. Jayne, 2007: Response of a climate model to tidal mixing parameterization under present day and Last Glacial Maximum conditions. *Ocean Modelling*, **19**, 125–137 doi:10.1016/j.ocemod.2007.06.009.

Munk, W. H. and C. Wunsch, 1998: Abyssal recipes II: Energetics of tidal and wind mixing. *Deep-Sea Res.*, **45**, 1977–2010.

Ohkouchi, N., H. Kawahata, M. Murayama, M. Okada, T. Nakamura and A. Taira, 2002: Was deep water formed in the North Pacific during the late Quaternary? Cadmium evidence from the northwest Pacific. *Earth and Planetary Science Letters*, **124**, 185–194.

Orsi, A. H., S. S. Jacobs, A. L. Gordon and M. Visbeck, 2001: Cooling and Ventilating the Abyssal Ocean. *Progress in Oceanography*, **28**, 2923–2926.

Orsi, A. H., G. C. Johnson and J. L. Bullister, 1999: Circulation, mixing and production of Antarctic Bottom Water. *Progress in Oceanography*, **43**, 55–109.

Pacanowski, R., 1995: *MOM2 Documentation User's Guide and Reference Manual: GFDL Ocean Group Technical Report*. NOAA, GFDL. Princeton. 232pp.

Peltier, W. R., 1994: Ice age paleotopography. *Science*, **265**, 195–201.

Phipps, S. J., L. D. Rotstayn, H. B. Gordon, J. L. Roberts, A. C. Hirst and W. F. Budd, 2011: The CSIRO Mk3L climate system model version 1.0 - Part 1: Description and evaluation. *Geosci. Model Dev. Discuss.*,, **4**, doi:10.5194/gmdd–4–219–2011 219–287.

Prange, P., G. Lohmann and A. Paul, 2001: The glacial thermohaline circulation: Stable or unstable? *Geophysical Research Letters*, **29**, 2028.

Rahmstorf, S., 1993: A fast and complete convection scheme for ocean models. *Ocean Modelling*, **101**, 9–11.

Rahmstorf, S., 1996: On the freshwater forcing and transport of the Atlantic thermohaline circulation. *Climate Dynamics*, **12**, 799–811.

Rahmstorf, S., 2002: Ocean circulation and climate during the past 120,000 years. *Nature*, **419**, 207–214.

Rahmstorf, S., M. Crucifix, A. Ganopolski, H. Goosse, I. Kamenkovich, K. R., G. Lohmann, R. Marsh, L. Mysak, Z. Wang and A. Weaver, 2005: Thermohaline circulation hysteresis: A model intercomparison. *Geophysical Research Letters*, **32**, L23 605, doi:10.1029/2005GL023 655.

Rahmstorf, S. and M. H. England, 1997: On the influence of Southern Hemisphere winds on North Atlantic Deep Water flow. *Journal of Physical Oceanography*, **27**, 2040–2054.

Ramillien, G., A. Lombard, A. Cazenave, E. R. Ivins, M. Llubes, F. Remy and R. Biancale, 2006: Interannual variations of the mass balance of the Antarctica and Greenland ice sheets from GRACE. *Global and Planetary Change*, **53**, 198–208.

Rignot, E., M. Bamber, J. Van den Broeke, M. Davis, Y. Li, W. van de Berg and E. van Mejigaard, 2008: Recent Antarctic ice mass loss from radar interferometry and regional climate modelling. *Nature Geoscience*, **1**, 106–110.

Rintoul, S. R., 2007: Rapid freshening of Antarctic Bottom Water formed in the Indian and Pacific oceans. *Geophysical Research Letters*, **34**, doi:10.1029/2006GL028 550.

Rohling, K. G., M. Bolshaw, A. P. Roberts, M. Siddall, C. Hemleben and M. Kucera, 2009: Antarctic temperature and global sea level closely coupled over the past five glacial cycles. *Nature Geoscience*, doi:10.1038/NGE0557.

Saenko, A., O. Schmittner and A. J. Weaver, 2004: The Atlantic-Pacific seesaw. *Journal of climate*, **17**, 2033–2038.

Saenko, O. A., J. M. Gregory, A. J. Weaver and M. Eby, 2002: Distinguishing the influences of heat, freshwater and momentum fluxes on ocean circulation and climate. *Journal of Physical Oceanography*, **32**, 3376–3395.

Saenko, O. A., A. Schmittner and A. J. Weaver, 2004: The Atlantic-Pacific seesaw. Journal of Climate. *Journal of Climate*, **17**, 2033–2038.

Saenko, O. A. and A. J. Weaver, 2001: Importance of wind-driven sea ice motion for the formation of Antarctic Intermediate Water in a global climate model. *Geophysical Research Letters*, **28**, 4147–4150.

Saenko, O. A., A. J. Weaver and J. M. Gregory, 2003: On the link between the two modes of the ocean thermohaline circulation and the formation of global-scale water masses. *Journal of Climate*, **16**, 2797–2801.

Sen Gupta, A. and M. H. England, 2007: Coupled ocean-atmosphere feedback in the Southern Annular Mode. *Journal of Climate*, **20**, 3677–3692 doi: 10.1175/JCLI4200.1.

Sen Gupta, A., A. Santoso, A. S. Taschetto, C. C. Ummenhofer, J. Trevena and M. H. England, 2008: Projected Changes to the Southern Hemisphere Ocean and Sea Ice in the IPCC AR4 Climate Models. *Journal of Climate*, **22**, doi: 10.1175/2008JCLI2827.1 3047–3075.

Shepherd, A., D. Wingham and E. Rignot, 2004: Warm ocean is eroding West Antarctic ice sheet. *Geophysical Research Letters*, **31**, 1–4.

Sijp, W. P. and M. H. England, 2005: On the role of the Drake Passage in controlling the stability of the ocean's thermohaline circulation. *Journal of Climate*, **18**, 1957–1966.

Sijp, W. P. and M. H. England, 2006: Sensitivity of the Atlantic Thermohaline Circulation and its stability to basin-scale variations in vertical mixing. *Journal of Climate*, **19**, 5467–54 781.

Sijp, W. P. and M. H. England, 2009: Southern Hemisphere Westerly wind control over the ocean's thermohaline circulation. *Journal of Climate*, **22**, 1277–1286.

Silvestri, G. E. and C. S. Vera, 2003: Antarctic Oscillation signal on precipiation anomalies over southeastern South America. *Geophysical Research Letters*, **30**, 2115 doi:10.1029/2003GL018 277.

Simmons, H. L., S. R. Jayne, L. C. St. Laurent and A. J. Weaver, 2003: Tidally driven mixing in a numerical model of the ocean general circulation. *Ocean Modelling*, **6**, 245–263 doi: 10.1016/S1463–5003(03)00 011–8.

Stanford, J. D., E. J. Rohling, S. E. Hunter, A. P. Roberts, S. O. Rasmussen, E. Bard, J. McManus and R. G. Fairbanks, 2006: Timing of meltwater pulse 1a and climate responses to meltwater injections. *Paleooceanography*, **21**, PA4103.

Stommel, H., 1961: Thermohaline Convection with two stable regimes of flow. *Tellus*, **13**, 224–230.

Stouffer, R. J. and S. Manabe, 2003: Equilibrium response of thermohaline circulation to large changes in atmospheric CO_2 concentration. *Climate Dynamics*, **20**, 759–773.

Stouffer, R. J., D. Seidov and B. Haupt, 2007: Climate Response to External Sources of Freshwater: North Atlantic versus the Southern Ocean. *Journal of Climate*, **20**, 436–448.

Talley, L. D., J. L. Reid and P. E. Robbins, 2003: Data-based meridional overturning streamfunctions for the global ocean. *Journal of Climate*, **16**, 3213–3226.

Thomas, R. H., 1979: The dynamics of marince ice sheets. *Journal of Glaciology*, **24**, 167–177.

Thompson, D. W. J. and J. M. Wallace, 2000: Annular modes in the extratropical circulation. Part I: Month-to-month variability. *Journal of Climate*, **13**, 1000–1016.

Toggweiler, J. R., J. L. Russell and S. R. Carson, 2006: Midlatitude westerlies, atmospheric CO_2 and climate change during the ice ages. *Paleoceanography*, **21**, doi: 10.1029 2005PA001 154.

Toggweiler, J. R. and B. L. Samuels, 1993: New radiocarbon constraints on the upwelling of abyssal water in the ocean's surface. *The Global Carbon Cycle, Springer-Verlag*, 333–366.

Toggweiler, J. R. and B. L. Samuels, 1995: Effect of Drake Passage on the global thermohaline circulation. *Deep-Sea Research I*, **42**, 477–500.

Trevena, J., W. P. Sijp and M. H. England, 2008: Southern Ocean response to freshwater anomalies and the effect on global climate. *Journal of Climate*, **21**, 3310–3326 doi: 10.1175/2007JCLI2212.1.

Velicogna, I. and J. Wahr, 2006: Measurements of Time-Variable Gravity show mass loss in Antarctia. *Science*, **311**, doi: 10.1126/science.1123 685. 1754.

Vellinga, M. and R. A. Wood, 2002: Global Climatic Impacts of a collapse of the Atlantic thermohaline circulation. *Climatic Change*, **54**, 251–267.

Weaver, A. J., M. Eby, E. C. Wiebe, C. M. Bitz, P. B. Duffy, T. L. Ewen, A. F. Fanning, M. M. Holland, A. MacFadyen, H. D. Matthews, K. J. Meissner, O. Saenko, A. Schmittner, H. Wang and M. Yoshimori, 2001: The UVic Earth System Climate Model: Model Description, Climatology and Applications to Past, Present and Future Climates. *Atmosphere-Ocean*, **39**, 0–00.

Weaver, A. J., O. A. Saenko, P. U. Clark and J. X. Mitrovica, 2003: Meltwater pulse 1a from Antarctica as a trigger of the Bolling-Allerod warm interval. *Science*, **299**, 1709–1713.

Wijffels, S. E., 2001: Ocean transport of fresh water. *Ocean Circulation and Climate: Observing and Modelling teh Global Ocean*,G. Sieler, J. church, and J. Gould, Eds. *International Geophysics Series*, **77**, 475–488.

Wingham, D., A. Shepherd, A. Muir and G. Marshall, 2006: Mass balance of the Antarctic ice sheet. *Philosophical Transactions of the Royal Society*, **364**, 1627–1635.

Yin, J., M. E. Schlesinger, N. G. Andronova, S. Malyshev and B. Li, 2006: Is a Shutdown of the Thermohaline Circulation Irreversible? *Journal of Geophysical Research*, **111**, D12 104, doi:10.1029/2005JD006 562.

Zwalley, H., M. B. Giovinetto, J. Li, H. Cornejo, M. A. Beckley, A. Brenner, J. Saba and D. Yi, 2005: Mass changes of the Greenland and Antarctic ice sheets and shelves and contributions to sea level rise. *Journal of Glaciology*, **51**, 509–527.